Early season depletion of dissolved iron in the Ross Sea polynya: Implications for iron dynamics on the Antarctic continental shelf

P. N. Sedwick,[1] C. M. Marsay,[2] B. M. Sohst,[1] A. M. Aguilar-Islas,[3] M. C. Lohan,[4] M. C. Long,[5,6] K. R. Arrigo,[5] R. B. Dunbar,[5] M. A. Saito,[7] W. O. Smith,[8] and G. R. DiTullio[9]

Received 27 July 2010; revised 12 September 2011; accepted 26 September 2011; published 15 December 2011.

[1] The Ross Sea polynya is among the most productive regions in the Southern Ocean and may constitute a significant oceanic CO_2 sink. Based on results from several field studies, this region has been considered seasonally iron limited, whereby a "winter reserve" of dissolved iron (dFe) is progressively depleted during the growing season to low concentrations (~0.1 nM) that limit phytoplankton growth in the austral summer (December–February). Here we report new iron data for the Ross Sea polynya during austral summer 2005–2006 (27 December–22 January) and the following austral spring 2006 (16 November–3 December). The summer 2005–2006 data show generally low dFe concentrations in polynya surface waters (0.10 ± 0.05 nM in upper 40 m, n = 175), consistent with previous observations. Surprisingly, our spring 2006 data reveal similar low surface dFe concentrations in the polynya (0.06 ± 0.04 nM in upper 40 m, n = 69), in association with relatively high rates of primary production (~170–260 mmol C m^{-2} d^{-1}). These results indicate that the winter reserve dFe may be consumed relatively early in the growing season, such that polynya surface waters can become "iron limited" as early as November; i.e., the seasonal depletion of dFe is not necessarily gradual. Satellite observations reveal significant biomass accumulation in the polynya during summer 2006–2007, implying significant sources of "new" dFe to surface waters during this period. Possible sources of this new dFe include episodic vertical exchange, lateral advection, aerosol input, and reductive dissolution of particulate iron.

Citation: Sedwick, P. N., et al. (2011), Early season depletion of dissolved iron in the Ross Sea polynya: Implications for iron dynamics on the Antarctic continental shelf, *J. Geophys. Res.*, *116*, C12019, doi:10.1029/2010JC006553.

1. Introduction

[2] Primary production that occurs in waters upwelled south of the Antarctic Polar Front is thought to play a critical role in regulating the air-sea flux of carbon dioxide. In essence, the magnitude of the Southern Ocean CO_2 sink depends on the biological drawdown of nutrients from these waters prior to the formation and subduction of deep waters around the Antarctic continent [*Marinov et al.*, 2006]. In this context, the Antarctic continental margin is of critical importance, being the most productive region in the Southern Ocean [*Arrigo et al.*, 2008a; *Smith and Comiso*, 2008] and a primary area of oceanic deep water formation [*Orsi et al.*, 2002; *Orsi and Wiederwohl*, 2009]. The Ross Sea continental shelf is among the most productive areas on the Antarctic margin [*Arrigo et al.*, 2008a; *Smith and Comiso*, 2008] and likely represents an important but unquantified oceanic CO_2 sink. Indeed, a modeling study by *Arrigo et al.* [2008b] suggests that the net air-sea CO_2 flux on the Ross Sea Shelf may account for as much as 27% of a recent estimate of the total Southern Ocean CO_2 sink, which does not include the Antarctic continental margin [*Takahashi et al.*, 2009]. An essential component of the Ross Sea CO_2 sink is provided by the regional phytoplankton production, which draws down pCO_2 in surface waters and drives the export of organic carbon to depth.

[3] The factors that control primary production in the Ross Sea are not completely understood, but are almost certain to include the availability of dissolved iron (dFe), at least during

[1]Deparment of Ocean, Earth and Atmospheric Sciences, Old Dominion University, Norfolk, Virginia, USA.
[2]School of Ocean and Earth Science, University of Southampton, Southampton, UK.
[3]School of Fisheries and Ocean Sciences, University of Alaska Fairbanks, Fairbanks, Alaska, USA.
[4]School of Earth, Ocean and Environmental Sciences, University of Plymouth, Plymouth, UK.
[5]Department of Environmental Earth System Sciences, Stanford University, Stanford, California, USA.
[6]Now at the National Center for Atmospheric Research, Boulder, Colorado, USA.
[7]Woods Hole Oceanographic Institution, Woods Hole, Massachusetts, USA.
[8]Virginia Institute of Marine Science, College of William and Mary, Gloucester Point, Virginia, USA.
[9]Grice Marine Laboratory, College of Charleston, Charleston, South Carolina, USA.

0148-0227/11/2010JC006553

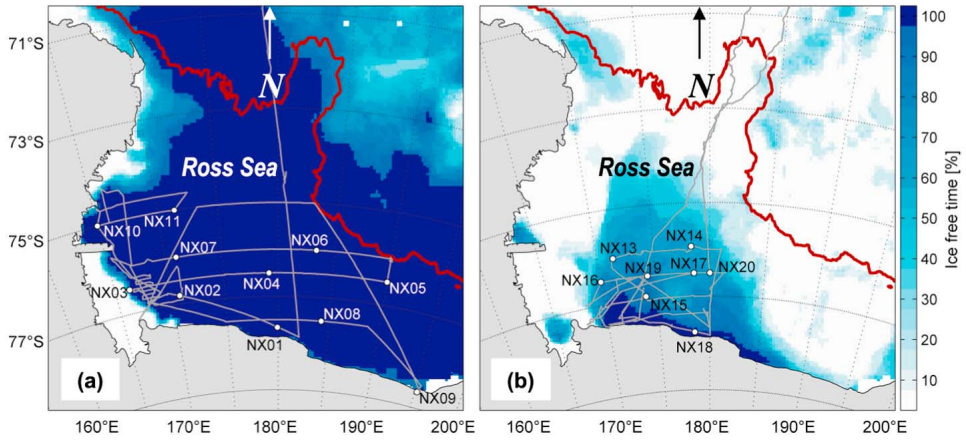

Figure 1. Cruise tracks and locations of trace-metal water column sampling stations during the CORSACS program, overlain on satellite-derived estimates of percentages of ice-free time during each cruise for (a) summer 2005–2006 and (b) spring 2006 (not shown is station NX12, located north of map area). The red line indicates the 1000 m isobath.

the latter part of the growing season [*Martin et al.*, 1991; *Sedwick et al.*, 2000; *Boyd*, 2002; *Coale et al.*, 2005]. In the highly productive polynya region of the southern Ross Sea, shipboard bioassay experiments have demonstrated that low dFe concentrations can limit phytoplankton growth rates during the austral summer [*Martin et al.,* 1990; *Sedwick and DiTullio*, 1997; *Sedwick et al.*, 2000, *Coale et al.*, 2003; *Bertrand et al.,* 2007]. When considered together, the limited iron data from the southern Ross Sea suggest that near-surface dFe concentrations decrease from ~0.2–1 nM in austral spring (September–November) to ~0.1–0.2 nM in austral summer (December–February) [*Fitzwater et al.*, 2000; *Sedwick et al.*, 2000; *Coale et al.,* 2005]. Over this same period, the surface concentrations of nitrate and silicic acid typically decrease from ~30 to ~15 μM and from ~80 to ~60 μM, respectively [*Smith et al.,* 2003].

[4] Based on these observations, it has been argued that the southern Ross Sea exhibits "seasonal iron limitation," whereby vertical resupply from convective mixing and surface inputs from melting sea ice result in relatively high dFe concentrations in surface waters during the spring, followed by a progressive decrease in dFe concentrations during the course of the growing season, because of the combined effects of phytoplankton uptake, particle export, and scavenging [*Sedwick et al.*, 2000; *Coale et al.*, 2005]. With these assumptions, numerical modeling has simulated the seasonal drawdown in dissolved iron and macronutrients, and the associated onset of "iron limitation" of phytoplankton growth rates and biomass, with model solutions indicating that the total supply of dissolved iron to waters in the euphotic zone sets an upper limit on the magnitude of annual primary production on the Ross Sea shelf [*Arrigo et al.*, 2003; *Tagliabue and Arrigo*, 2005].

[5] In this paper we report new measurements that reveal surprisingly low dFe concentrations (~0.1 nM) in the euphotic zone of the Ross Sea polynya in late spring (November), thus challenging the conceptual model of gradual dFe depletion during the growing season and raising questions concerning the source of "new" dissolved iron that sustains phytoplankton production over the ensuing summer months. As discussed by *Boyd and Ellwood* [2010], iron exhibits both "nutrient-type" and "scavenged-type" behavior in the oceanic water column. In remote regions of the open ocean, such as the Antarctic Circumpolar Current, this hybrid behavior results in chronic iron deficiency whereby upwelled subsurface waters contain an excess of macronutrients over dissolved iron, relative to the nutritional requirements of phytoplankton. A critical difference between iron and macronutrients is the clear importance of aeolian and benthic sources of iron to the surface ocean [*Moore and Braucher*, 2008; *Boyd and Ellwood*, 2010]. In the Ross Sea, benthic inputs are likely to be particularly important, both in terms of the vertical resupply of iron during winter mixing and in the potential for episodic vertical and lateral inputs of iron to surface waters of the polynya during summer. Bearing this in mind, we examine our new data with particular attention to potential sources of dissolved iron to both surface and subsurface waters of the southern Ross Sea.

2. Methods

[6] The data presented in this paper pertain to samples collected during two cruises aboard the research vessel ice breaker (RVIB) *Nathaniel B. Palmer*, as part of the Controls on Ross Sea Algal Community Structure (CORSACS) program. Water samples discussed here were collected in the austral summer of 2005–2006 (27 December 2005–22 January 2006, during cruise NBP06–01) and during the following austral spring of 2006 (8 November 2006–3 December 2006, during cruise NBP06–08). Figures 1a and 1b show the cruise tracks and trace-metal water column sampling stations (except station NX12, which was located north of the Ross Sea) overlain on satellite-derived estimates of ice-free time during each cruise, which were obtained using the method of *Markus and Burns* [1995].

[7] Hydrographic data and samples for ancillary chemical and biological measurements (salinity, dissolved oxygen, macronutrients, phytoplankton pigments, primary productivity) were collected using a rosette sampler fitted with 24 10 L Niskin bottles (General Oceanics), an SBE 911 *plus* conductivity, temperature, and depth (CTD) sensor (SeaBird Electronics), an SBE 43 dissolved oxygen sensor, and a

WETStar flow-through profiling fluorometer (WET Labs). The dissolved oxygen sensor was calibrated based on discrete dissolved oxygen measurements, as described by *Long et al.* [2011a]. The profiling fluorometer was not calibrated at sea; thus the raw signal output provides only a qualitative measure of water column chlorophyll levels. Further details and data for these ancillary measurements are provided by *Long et al.* [2011a] and archived at the U.S. Biological and Chemical Oceanography Data Management Office (see section 3).

[8] Seawater samples for the analysis of trace metals were collected using two methods: (1) Near-surface seawater samples were collected from ~3 m depth while underway at a speed of ~5 knots, using a towed, trace-metal-clean pumping system [*Bruland et al.*, 2005]; and (2) water column samples were collected in custom-modified 5 L Teflon-lined, external-closure Niskin-X samplers (General Oceanics) or in 10 L Teflon-lined GO-FLO samplers (General Oceanics; >300 m depth samples only), all of which were deployed on a nonmetal line [*Sedwick et al.*, 2005; *Saito et al.*, 2010]. Figures 2a and 2b show the location of the near-surface underway samples and the water column trace-metal sampling stations, overlain on ETOPO1 bathymetry [*Amante and Eakins*, 2008]. The extensive sea ice cover during the spring 2006 cruise restricted the underway and water column sampling to a much smaller area of the Ross Sea than that sampled during the summer 2005–2006 cruise.

[9] All seawater samples were filtered within 4 h of collection using 0.2 μm pore Supor Acropak filter capsules (Pall Corp.), except for the GO-FLO samples, which were filtered through 0.4 μm pore, 144 mm diameter polycarbonate filter membranes (GE Osmonics). All filtered seawater samples were acidified to pH 1.7 with Seastar Baseline ultrapure hydrochloric acid and then stored for at least 24 h prior to the analysis of dissolved iron. Dissolved iron (dFe) was determined by flow injection analysis with colorimetric detection after an in-line preconcentration on resin-immobilized 8-hydroxyquinoline [*Sedwick et al.*, 2005, 2008], using a method modified from *Measures et al.* [1995]. The efficacy of our sample collection, processing, and analytical methods for dFe have been verified through participation in the Sampling and Analysis of Iron (SAFe) intercomparison exercise for the sampling and analysis of iron in seawater [*Johnson et al.*, 2007]. For the SAFe seawater reference materials, we determined mean dFe concentrations of 0.11 ± 0.01 nM (for surface seawater S1, n = 15) and 0.97 ± 0.06 nM (for deep seawater D2, n = 14), compared with the SAFe community consensus values of 0.097 ± 0.043 nM (for seawater S1) 0.91 ± 0.17 nM (for seawater D2).

[10] In addition, unfiltered aliquots of the water column samples were acidified to pH 1.7 with Seastar Baseline ultrapure hydrochloric acid and then stored for at least 6 months, prior to determination of "total-dissolvable iron" (TDFe) by flow injection analysis using the same method as for dFe. TDFe is equal to the concentration of dFe plus acid-labile particulate iron (ALPFe). The latter is assumed to include most of the particulate iron in seawater, with the exception of lattice-bound iron in refractory aluminosilicate particles, which likely does not participate in the marine iron cycle over seasonal to annual time scales. Thus ALPFe (=TDFe – dFe) provides a conservative estimate of particulate iron in the water column. Dissolved inorganic nitrate plus nitrite (N + N), phosphate (DIP), and silicic acid (Si) were determined in filtered seawater samples with a shipboard Lachat Quickchem FIA+ series 8000 autoanalyzer following a method modified from standard World Ocean Circulation Experiment (WOCE) protocols [*Gordon et al.*, 1993].

3. Results

[11] Iron data from the two CORSACS cruises are presented in Figures 2–5. Figures 2a and 2b show dFe concentrations in near-surface underway samples from the summer 2005–2006 and spring 2006 cruises, respectively. Figures 3 and 4 show water column dFe concentration profiles from the summer 2005–2006 and spring 2006 cruises, respectively. Figure 5 presents quasi-zonal sections of dFe, dissolved nitrate plus nitrite (N + N), and total-dissolvable iron (TDFe) that were constructed by interpolating between vertical profiles from sampling stations located within the latitudinal band of 76°S–77°S. The corresponding hydrographic data (temperature, salinity, dissolved oxygen) from CTD stations along this quasi-zonal section are presented in Figure 6. The zonal plots shown in Figures 5 and 6 were prepared using the Ocean Data View graphical analysis and display package [*Schlitzer*, 2002], with interpolation performed using horizontal scale settings of 30 (for Figure 5) and 70 (for Figure 6), and a vertical scale setting of 70. A lower horizontal scale setting was chosen for Figure 5 in order to limit the extent of lateral interpolation, given that the trace-metal sampling stations were widely spaced relative to the CTD stations that provided the data shown in Figure 6.

[12] Table 1 presents the sampling dates, station locations, estimated mixed-layer depths, and iron (dFe, TDFe, calculated ALPFe) and macronutrient (N + N, DIP, Si) data for the trace-metal water column sampling stations. In addition, these and ancillary data discussed in this paper (hydrography, nutrients, iron, pigments) are archived at and freely available from the U.S. Biological and Chemical Oceanography Data Management Office (see http://osprey.bcodmo.org/project.cfm under project acronym CORSACS). The water masses discussed in this paper follow the classification scheme of *Orsi and Wiederwohl* [2009], who describe six distinct water masses over the Ross Sea continental shelf: the low-salinity Antarctic Surface Water (AASW); the relatively warm, oxygen-poor Modified Circumpolar Deep Water (MCDW); the relatively cold Shelf Water (SW), which includes both Low-Salinity Shelf Water (LSSW) and High-Salinity Shelf Water (HSSW); the transitional Modified Shelf Water (MSW); and the very cold Ice Shelf Water (ISW).

3.1. Summer 2005–2006 Cruise

[13] The summer 2005–2006 cruise was characterized by largely ice-free conditions (<10% sea ice coverage) over most of the southern Ross Sea (Figure 1a). Shipboard observations revealed significant lateral gradients in mixed-layer depth, surface macronutrient concentrations, phytoplankton biomass, and primary productivity, with the greatest macronutrient drawdown observed in the shallow mixed layers adjacent to sea ice along the western edge of our study area [*Long et al.*, 2011a]. Waters in the surface

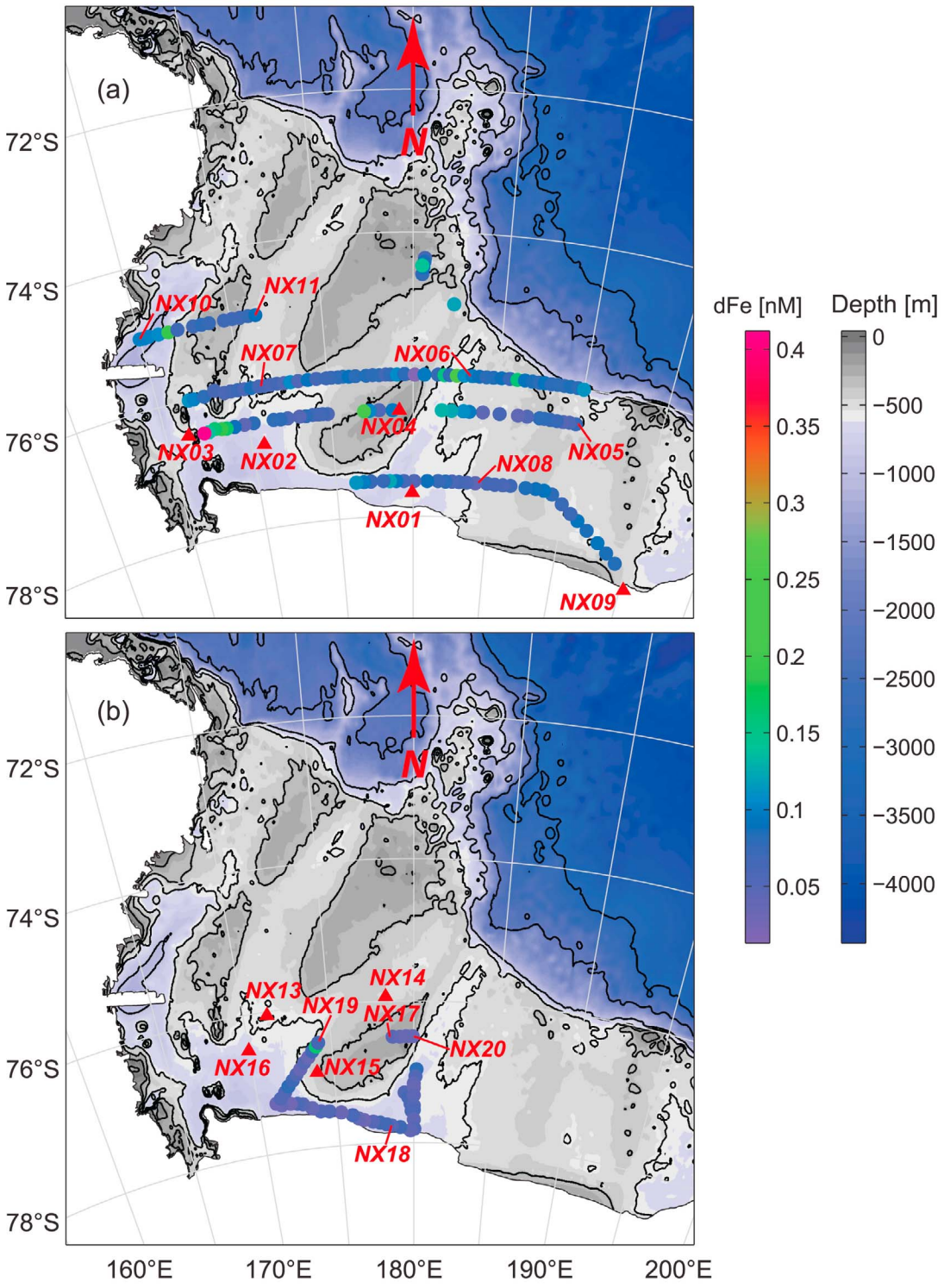

Figure 2. Maps of study area showing dissolved iron (dFe) concentrations of near-surface underway seawater samples from (a) summer 2005–2006 and (b) spring 2006, along with the locations of trace-metal water column sampling stations (NX12 not shown) and ETOPO1 seafloor bathymetry.

mixed layer were generally replete in macronutrients, with N + N concentrations of ~10–25 μM measured at most stations. Phytoplankton assemblages were typically dominated by mixtures of *Phaeocystis antarctica* and diatoms [*Long et al.*, 2011a; *Tortell et al.*, 2011].

[14] Iron data from the summer 2005–2006 cruise are consistent with previous observations from the southern Ross Sea, in that dFe concentrations were generally low in the surface mixed layer. Our underway samples reveal near-surface dFe concentrations of less than 0.2 nM over most of

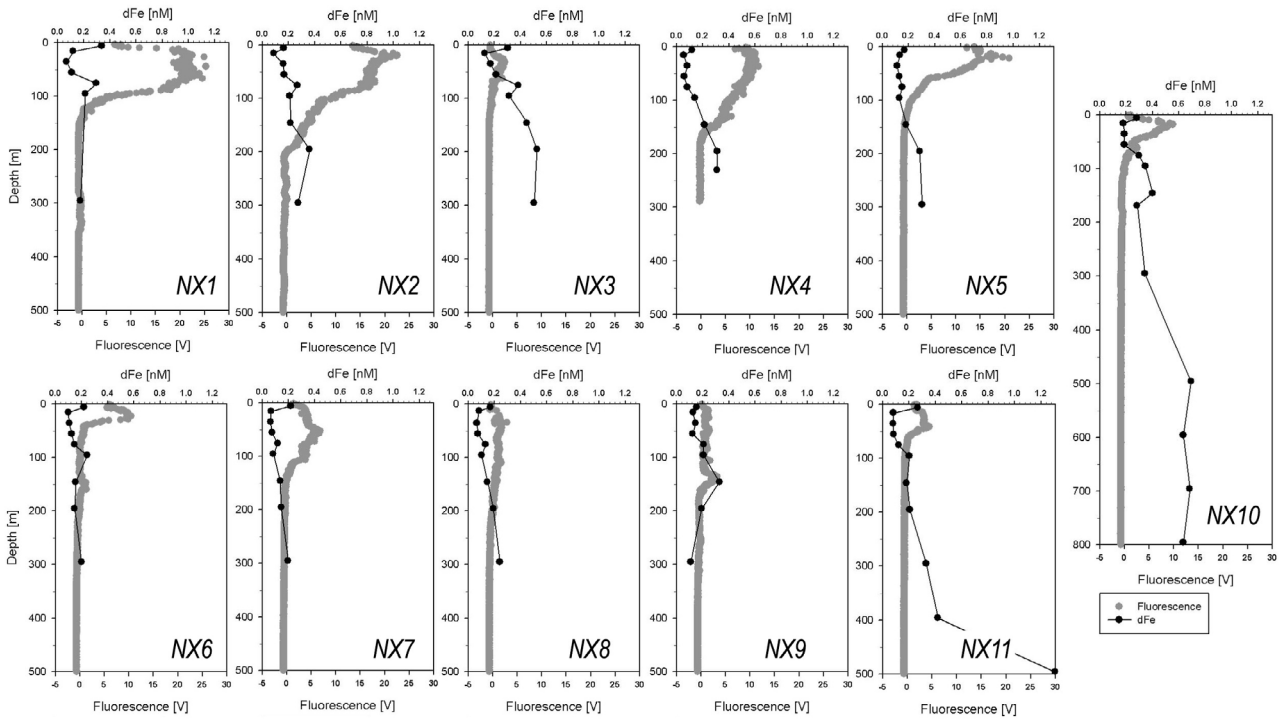

Figure 3. Vertical profiles of dissolved iron (dFe) concentrations and in situ chlorophyll fluorescence (uncalibrated fluorometer signal) at trace-metal sampling stations from the summer 2005–2006 cruise.

the polynya (Figure 2a). Corresponding water column profiles show similarly low dFe concentrations to depths of ~100 m in the central polynya, with slightly elevated concentrations (0.2–0.3 nM) in near-surface waters toward the eastern and western edges of the polynya (Figures 2a, 3, and 5c). The zonal distribution of dFe in the euphotic zone along 76°S–77°S (Figure 5c) is qualitatively similar to that observed for N + N (Figure 5e), implying that surface dFe concentrations are strongly influenced by algal iron uptake. This conclusion is further supported by the vertical profiles of dFe and chlorophyll fluorescence (Figure 3), which display opposing trends in the upper water column (Figure 3), assuming that chlorophyll fluorescence provides a rough gauge of phytoplankton biomass. Further, the clear depletion of TDFe, hence acid-labile particulate Fe, in the upper water column relative to deeper waters (Figure 5g and Table 1) indicates that both dissolved and particulate iron had been exported from the euphotic zone prior to our sampling. The presence of subtle surface maxima in dFe, particularly toward the western and eastern edges of the polynya (Figures 2a, 3, and 5c), suggests surface iron inputs from melting sea ice, consistent with the lower salinity of surface waters west of 170°E and east of 180° (Figure 6e).

[15] Along 76°S–77°S, the vertical profiles from stations NX3, NX4, and NX5 reveal subsurface dFe maxima of ~0.3–0.5 nM at depths of 150–300 m (Figures 3 and 5c). A comparison of the zonal dFe section in Figure 5c with corresponding sections for N + N (Figure 5e), TDFe (Figure 5g), temperature (Figure 6c), and salinity (Figure 6e) suggests that these three dFe maxima may reflect inputs from three distinct sources of iron to subsurface waters of the Ross Sea. The subsurface dFe maximum at station NX3 appears to be associated with the core of relatively cold, salty, oxygen- and nitrate-rich water, which notably lacks a corresponding maximum in TDFe (Figure 5g) and hence ALPFe (Table 1). These hydrographic characteristics and location are indicative of SW, which is believed to form in coastal polynyas along the western Ross Ice Shelf and in Terra Nova Bay [*Orsi and Wiederwohl*, 2009]. The relatively high dFe and nitrate concentrations in this water mass will likely reflect the conditions in surface waters of the coastal polynyas where the SW forms. We observed similarly high dFe concentrations below 300 m depth at station NX10 in Terra Nova Bay (Figure 3), where hydrographic data (not shown) also reveal the presence of SW, although we did not collect deep-water samples for TDFe analysis at this location. These observations suggest that Ross Sea SW, which is thought to be an important contributor to Antarctic Bottom Water [*Orsi and Wiederwohl*, 2009], is characterized by relatively high dFe concentrations (~0.5–0.7 nM).

[16] The subsurface dFe maximum at station NX4 is located over Ross Bank, which shoals to a water depth of ~300 m (Figure 2a). Here the dFe maximum lies within the MSW, although it is not clearly associated with any regional hydrographic features (Figures 6c and 6e). Instead, this dFe maximum is distinguished by a pronounced associated maximum in TDFe (11–24 nM), relative to the subsurface TDFe concentrations of ~2–5 nM at other stations sampled during the cruise (Figure 5g). These elevated concentrations of TDFe, and hence ALPFe (Table 1), implicate seafloor sediments as the likely source of the subsurface dFe maximum at station NX4. A number of studies suggest that onshore flow is concentrated along the western flanks of submarine banks on the Ross Sea Shelf [*Hofmann and Klinck*, 1998; *Dinniman et al.*, 2003, 2011; *Reddy and Arrigo*, 2006], which provides a potential mechanism for

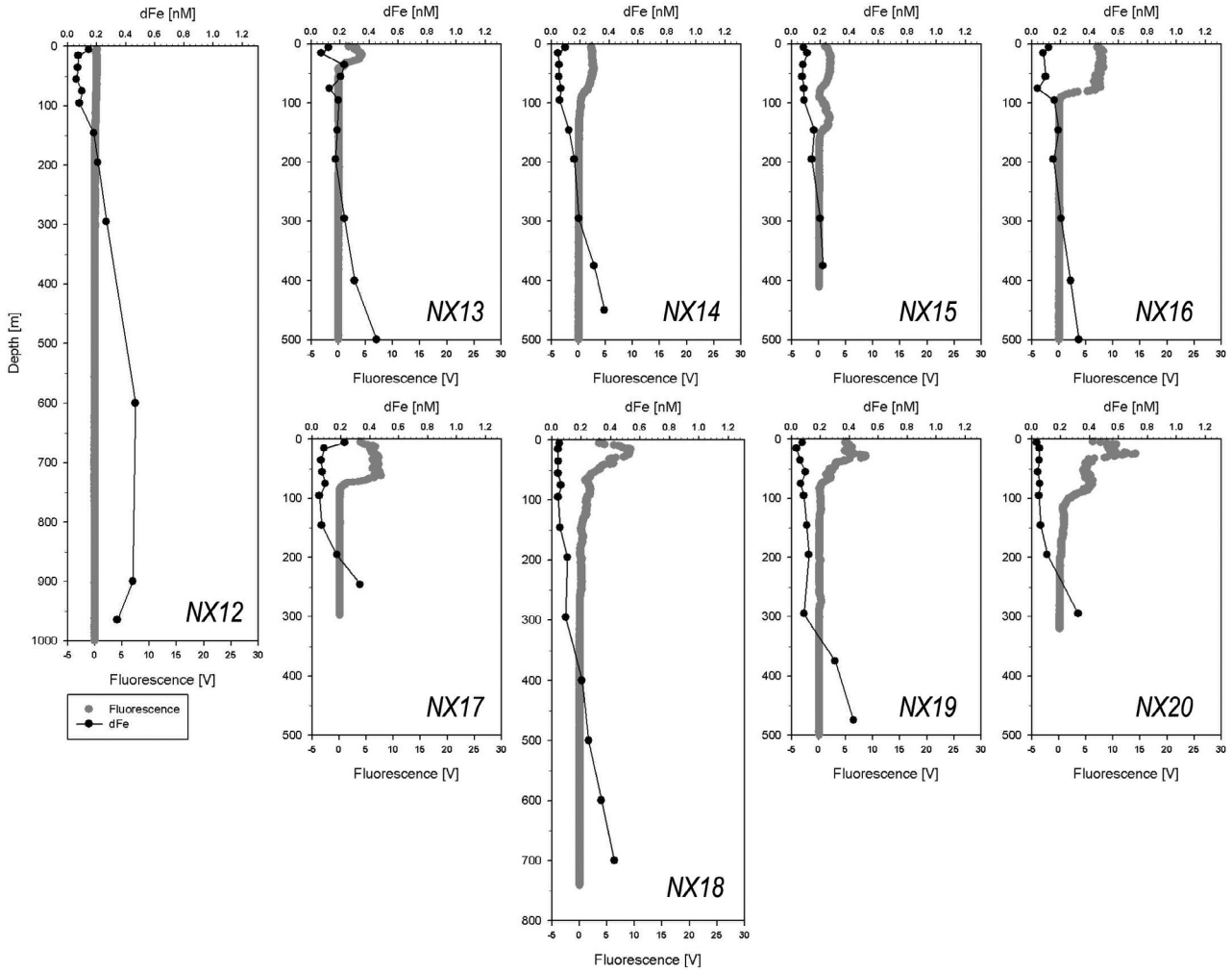

Figure 4. Vertical profiles of dissolved iron (dFe) concentrations and in situ chlorophyll fluorescence (uncalibrated fluorometer signal) at trace-metal sampling stations from the spring 2006 cruise.

mobilizing iron-bearing sediments from the Ross Bank into the overlying water column.

[17] Such onshore transport may serve to entrain MCDW [*Dinniman et al.,* 2003, 2011; *Orsi and Wiederwohl*, 2009], which has been proposed as a source of iron for surface waters on the Antarctic continental margins [*Prézelin et al.*, 2000, 2004; *Sambrotto et al.*, 2003; *Dinniman et al.*, 2011]. For MCDW to serve as a source of dFe to the inner shelf would require that the circumpolar deep water (CDW) end-member be inherently rich in dFe relative to Antarctic surface waters, or that MCDW intrusions mobilize iron-rich sediments and bottom waters through interactions with the seafloor on the continental slope or shelf. Our hydrographic data provide no evidence of MCDW at station NX4, where we see evidence of benthic inputs of dissolved and particulate iron. However, the subsurface dFe maximum at station NX5 (Figure 5c) is located at the edge of relatively warm, low-oxygen waters, which appear to reflect an intrusion of MCDW at ~300 m depth (Figures 6c and 6g). This interpretation would certainly be consistent with the Ross Sea climatology presented by *Orsi and Wiederwohl* [2009], who document frequent intrusions of MCDW in this depth range between longitudes 170°W and 175°W, as well as the recent model simulations reported by *Dinniman et al.* [2011]. The lack of a corresponding maximum in TDFe, and hence in ALPFe, in subsurface waters at station NX5 (Figure 5g) might then imply that CDW contributes dFe to the MCDW that impinges on the Ross Sea Shelf; i.e., the water column data from station NX5 suggest that MCDW derives dissolved iron (but not particulate iron) from CDW. Further support for this hypothesis is provided by the samples obtained at deep-ocean station NX12 (65°13′S, 174°44′W; location not shown in Figures 1 and 2) during the spring 2006 cruise (see below). These water column samples reveal a maximum dFe

Figure 5. (a, b) Locations of water column sampling stations used to construct quasi-zonal sections of dissolved iron (dFe) in (c) summer 2005–2006 and (d) spring 2006, nitrate plus nitrite (N + N) in (e) summer 2005–2006 and (f) spring 2006, and total-dissolvable iron (TDFe) in (g) summer 2005–2006 and (h) spring 2006. Gray triangles indicate approximate depth of seafloor; red frames in Figures 5c, 5g, and 5e indicate the lateral extent of the spring 2006 zonal section.

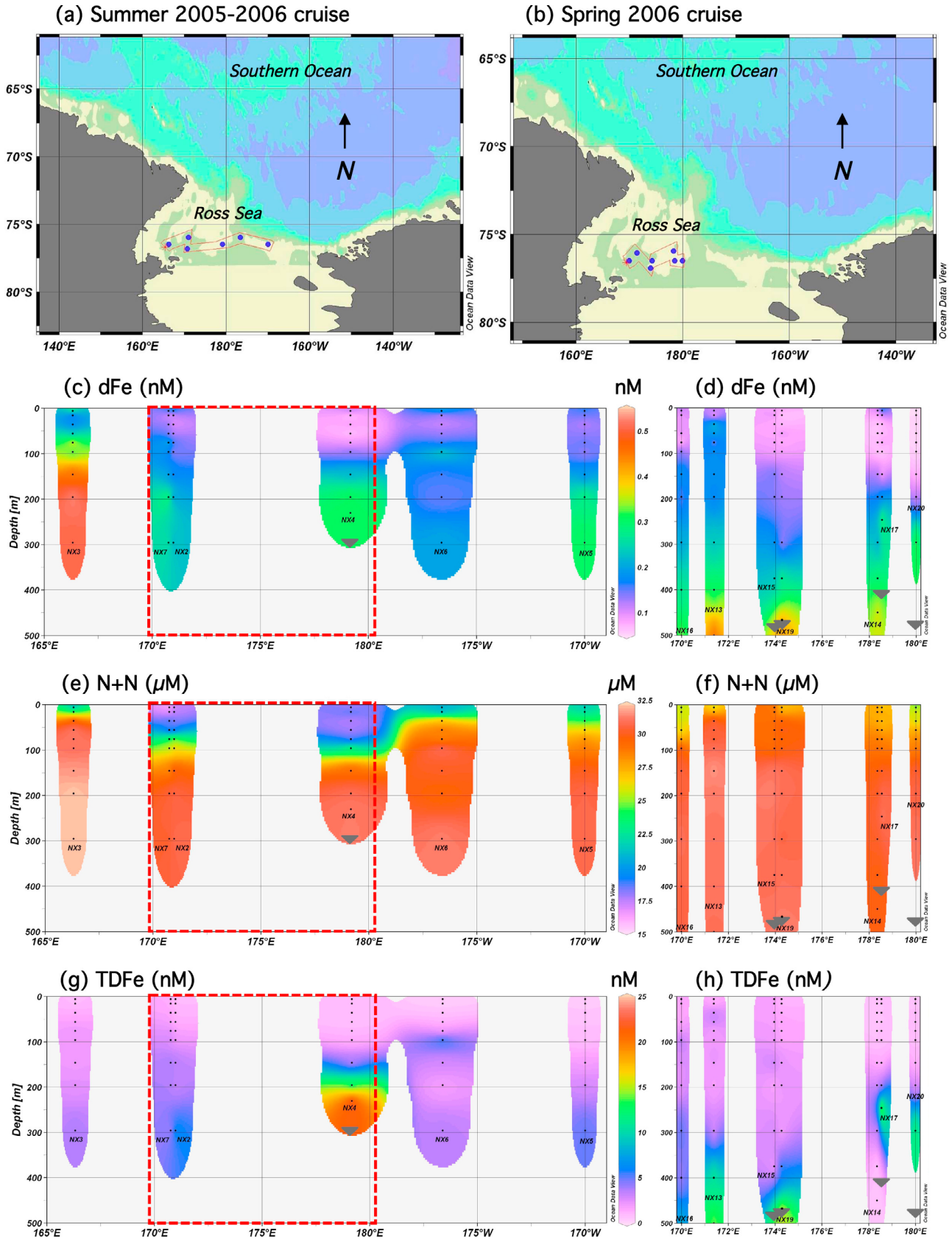
(a) Summer 2005-2006 cruise
(b) Spring 2006 cruise
Southern Ocean
Ross Sea
N
65°S
70°S
75°S
80°S
140°E
160°E
180°E
160°W
140°W
Ocean Data View
(c) dFe (nM)
(d) dFe (nM)
(e) N+N (μM)
(f) N+N (μM)
(g) TDFe (nM)
(h) TDFe (nM)
nM
μM
Depth [m]
NX3
NX7
NX2
NX4
NX6
NX5
NX16
NX13
NX15
NX19
NX14
NX17
NX20
165°E
170°E
175°E
180°E
175°W
170°W
172°E
174°E
176°E
178°E

Figure 5

concentration of ~0.5 nM within the salinity maximum that defines the core of the CDW north of the continental shelf (Figure 4), implying that CDW could contribute dFe to MCDW in the Ross Sea.

3.2. Spring 2006 Cruise

[18] The spring 2006 cruise was marked by extensive pack ice cover, with only a relatively small area of the southern Ross Sea having less than 10% sea ice coverage. This heavy sea ice cover confined the cruise track to a much smaller area compared with the preceding summer (Figure 1b). Satellite data show that the polynya opened more gradually than usual during spring, primarily driven by advection of sea ice rather than melting [*Long et al.*, 2011a, 2011b]. Surface properties were generally more homogeneous than during the preceding summer cruise, with a west-to-east decrease in surface salinity (Figure 6f), leading to greater stratification in the east of our study area. Macronutrients were replete at all stations sampled, with water column N + N concentrations generally in excess of 20 μM. Phytoplankton assemblages were dominated by colonial *Phaeocystis antarctica*, which appears to be a typical situation for the Ross Sea polynya during spring [*Long et al.*, 2011a; *Tortell et al.*, 2011; *Arrigo and van Dijken*, 2004; *Garrison et al.*, 2004].

[19] Our iron data from the spring 2006 cruise reveal dFe concentrations in surface waters of the polynya that were similar to or lower than values measured during the preceding summer, with dFe concentrations near or below 0.1 nM in most samples (Figure 2b). Moreover, the iron-deficient waters extended to depths below 100 m within the polynya (Figures 4 and 5d), which in some cases was deeper than the surface mixed layer at the time of sampling (Table 1). These observations are surprising, given that *Sedwick et al.* [2000] measured dFe concentrations of ~0.5–1 nM in surface waters of this region during November–December 1994, and *Coale et al.* [2005] report near-surface dFe levels of ~0.2–0.6 nM during October–November 1996. However, it is important to note that the data reported by *Sedwick et al.* [2000] are for samples collected at stations with ~50%–80% sea ice cover and that the data of *Coale et al.* [2005] are from a cruise when the sea surface was nearly completely ice covered. Because of the iron that is contained in both sea ice and overlying snow, sea ice meltwater may provide a significant input of dFe to surface waters of the Ross Sea [*Sedwick and DiTullio*, 1997; *Edwards and Sedwick*, 2001; *Grotti et al.*, 2005; *Lannuzel et al.*, 2007; *Lancelot et al.*, 2009]. Hence, near-surface waters sampled adjacent to sea ice, such as those described by *Sedwick et al.* [2000] and *Coale et al.* [2005], might be expected to display significantly elevated dFe concentrations. In contrast, our near-surface samples from the spring 2006 cruise were largely collected in ice-free waters of the polynya or during periods when sea ice was forming rather than melting. The only exceptions were at the deep-ocean station NX12 and the polynya station NX17, where some pack ice was present; at both stations, low surface salinities provide evidence of recent meltwater inputs and the near-surface dFe concentrations were slightly elevated relative to other stations (Figure 4 and Table 1).

[20] The southern Ross Sea is subject to deep convective mixing during the winter months [*Gordon et al.*, 2000], so it seems reasonable to assume that the dFe concentrations of ~0.3 nM observed at 400 m depth (Figure 5d) represent a likely minimum value for the "winter reserve" dFe concentration of surface waters at the start of the growing season in September–October. This assumption is consistent with the near-surface dFe values of 0.2–0.6 nM reported by *Coale et al.* [2005] for the southern Ross Sea in October–November 1996, which represent the only published iron data for this region during early spring. On this basis, the data shown in Figure 5d suggest that a substantial drawdown in dFe had occurred to depths of ~150–300 m in the central polynya, between 172°E and 180°E, by mid-November–early December. In comparison, the apparent biological drawdown in N + N was largely confined to the upper 100 m of the water column (Figure 5f). This apparent decoupling between the drawdown of dFe and nitrogen might reflect the elevated iron requirements of phytoplankton growing under low irradiance [*Raven*, 1990; *Sunda and Huntsman*, 1997; *Garcia et al.*, 2009], such that algal growth had depleted dFe relative to nitrate (i.e., high Fe/N assimilation ratio) in the deeper surface mixed layer of the early spring, prior to our sampling. An alternative hypothesis is that dFe, which is strongly particle reactive, had been scavenged by sinking particles (e.g., *Phaeocystis* aggregates) over the 100–300 m depth range [*Johnson et al.*, 1997; *DiTullio et al.*, 2000; *Moore et al.*, 2004; *Boyd and Ellwood*, 2010].

[21] A comparison of the zonal sections from the summer 2005–2006 (Figure 5c) and spring 2006 (Figure 5d) cruises suggests that dFe was depleted to greater depths in the central polynya during spring 2006 relative to the preceding summer. However, this conclusion must be considered as tentative, given the relatively wide spacing between sampling stations during the summer 2005–2006 cruise (Figure 5c). Bearing in mind the higher lateral resolution and greater sampling depths along this zonal section during spring 2006, our data reveal no major differences in the subsurface dFe distribution relative to the preceding summer cruise. Stations NX17 and NX20, located over Ross Bank, show maxima in dFe, TDFe, and ALPFe at ~250–300 m depth (Figures 4, 5d, and 5h and Table 1), suggesting benthic inputs of dissolved and particulate iron, as was suggested for station NX4. Similarly, deep maxima in dFe, TDFe and ALPFe at stations NX13 and NX19 (Figures 4, 5d, and 5h and Table 1) suggest iron inputs from seafloor sediments at these sites. Thus the water column data from both cruises provides evidence of benthic inputs of both dissolved and particulate iron close to the seafloor, although we find no evidence that these inputs are associated with intrusions of MCDW. Rather, our data suggest that MCDW may carry elevated concentrations of dissolved iron (but not particulate iron) that is derived from the CDW.

Figure 6. (a, b) Locations of water column sampling stations used to construct quasi-zonal sections of temperature (*T*) in (c) summer 2005–2006 and (d) spring 2006, salinity (*S*) in (e) summer 2005–2006 and (f) spring 2006, and dissolved oxygen (O_2, from CTD sensor) in (g) summer 2005–2006 and (h) spring 2006. Bathymetry shown (gray) is interpolated between bottom depths for CTD stations; the red frames shown in Figures 6c, 6g, and 6e indicate the lateral extent of the spring 2006 zonal section.

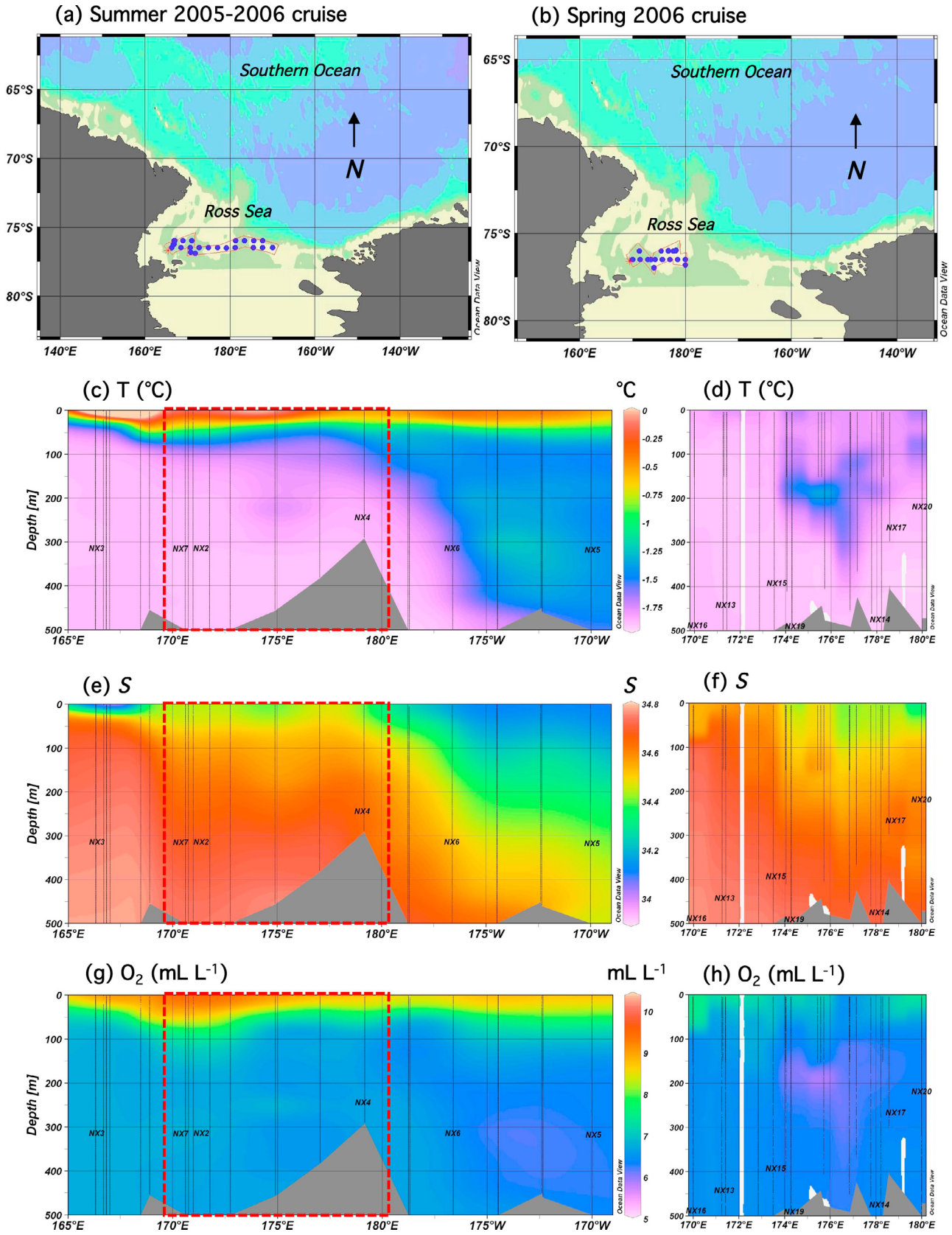
(a) Summer 2005-2006 cruise
(b) Spring 2006 cruise
Southern Ocean
Ross Sea
N
65°S
70°S
75°S
80°S
140°E
160°E
180°E
160°W
140°W
Ocean Data View
(c) T (°C)
(d) T (°C)
°C
(e) S
(f) S
S
(g) O2 (mL L-1)
(h) O2 (mL L-1)
mL L-1
Depth [m]
NX3
NX7
NX2
NX4
NX6
NX5
NX20
NX17
NX15
NX13
NX16
NX19
NX14
165°E
170°E
175°E
180°E
175°W
170°W
172°E
174°E
176°E
178°E

Figure 6

Table 1. Data From Trace-Metal Water Column Sampling Stations[a]

Station Name	Sampling Date	Latitude (°S)	Longitude (°E)	MLD[b] (m)	Depth (m)	dFe (nM)	TDFe (nM)	ALPFe[c] (nM)	N + N (μM)	DIP (μM)	Si (μM)
CORSACS-1 NX1	29 Dec 2005	77.67	179.94	ND	6	0.34	1.03	0.69	16.7	1.4	79.8
CORSACS-1 NX1	29 Dec 2005	77.67	179.94	ND	16	0.12	0.73	0.61	18.4	1.7	83.1
CORSACS-1 NX1	29 Dec 2005	77.67	179.94	ND	36	0.07	0.73	0.66	20.1	1.6	71.6
CORSACS-1 NX1	29 Dec 2005	77.67	179.94	ND	56	0.11	1.07	0.96	14.1	1.7	50.0
CORSACS-1 NX1	29 Dec 2005	77.67	179.94	ND	76	0.30	2.01	1.71	22.9	2.0	80.0
CORSACS-1 NX1	29 Dec 2005	77.67	179.94	ND	96	0.21	2.81	2.60	26.5	2.2	82.1
CORSACS-1 NX1	29 Dec 2005	77.67	179.94	ND	296	0.18	3.62	3.44	24.3	2.0	70.0
CORSACS-1 NX2	30 Dec 2005	76.82	170.76	56	6	0.17	1.75	1.59	15.2	1.4	79.4
CORSACS-1 NX2	30 Dec 2005	76.82	170.76	56	16	0.09	1.85	1.76	16.4	1.4	79.6
CORSACS-1 NX2	30 Dec 2005	76.82	170.76	56	36	0.16	2.19	2.03	19.3	1.6	79.7
CORSACS-1 NX2	30 Dec 2005	76.82	170.76	56	56	0.17	2.27	2.10	17.2	1.6	69.1
CORSACS-1 NX2	30 Dec 2005	76.82	170.76	56	76	0.27	3.32	3.05	24.0	1.9	81.4
CORSACS-1 NX2	30 Dec 2005	76.82	170.76	56	96	0.21	3.47	3.26	25.3	1.9	81.5
CORSACS-1 NX2	30 Dec 2005	76.82	170.76	56	146	0.22	4.00	3.78	27.4	2.0	81.6
CORSACS-1 NX2	30 Dec 2005	76.82	170.76	56	196	0.36	3.86	3.50	30.3	2.2	81.8
CORSACS-1 NX2	30 Dec 2005	76.82	170.76	56	296	0.28	2.85	2.58	29.9	2.1	78.2
CORSACS-1 NX3	1 Jan 2006	76.49	166.33	6	6	0.31	0.91	0.60	20.0	1.5	68.9
CORSACS-1 NX3	1 Jan 2006	76.49	166.33	6	16	0.13	0.78	0.66	25.0	2.0	74.1
CORSACS-1 NX3	1 Jan 2006	76.49	166.33	6	36	0.17	1.33	1.16	30.1	2.3	78.1
CORSACS-1 NX3	1 Jan 2006	76.49	166.33	6	56	0.22	1.55	1.33	31.4	2.2	78.7
CORSACS-1 NX3	1 Jan 2006	76.49	166.33	6	76	0.38	2.21	1.83	31.0	2.2	78.9
CORSACS-1 NX3	1 Jan 2006	76.49	166.33	6	96	0.32	1.81	1.50	31.0	2.3	79.6
CORSACS-1 NX3	1 Jan 2006	76.49	166.33	6	146	0.45	1.91	1.46	31.6	2.3	79.7
CORSACS-1 NX3	1 Jan 2006	76.49	166.33	6	196	0.53	2.36	1.83	32.2	2.3	80.6
CORSACS-1 NX3	1 Jan 2006	76.49	166.33	6	296	0.51	3.62	3.11	32.1	2.3	81.6
CORSACS-1 NX4	3 Jan 2006	76.50	179.17	60	6	0.12	0.85	0.73	17.8	1.4	74.9
CORSACS-1 NX4	3 Jan 2006	76.50	179.17	60	16	0.06	0.76	0.70	18.8	1.4	79.7
CORSACS-1 NX4	3 Jan 2006	76.50	179.17	60	36	0.08	0.67	0.59	17.5	1.4	74.5
CORSACS-1 NX4	3 Jan 2006	76.50	179.17	60	56	0.06	0.78	0.72	17.6	1.4	74.1
CORSACS-1 NX4	3 Jan 2006	76.50	179.17	60	76	0.08	0.87	0.79	17.6	1.4	74.0
CORSACS-1 NX4	3 Jan 2006	76.50	179.17	60	96	0.14	1.35	1.21	24.4	1.9	77.4
CORSACS-1 NX4	3 Jan 2006	76.50	179.17	60	146	0.22	2.80	2.58	29.2	2.2	79.5
CORSACS-1 NX4	3 Jan 2006	76.50	179.17	60	196	0.31	11.10	10.79	30.9	2.2	80.2
CORSACS-1 NX4	3 Jan 2006	76.50	179.17	60	231	0.31	24.26	23.95	31.2	2.2	81.2
CORSACS-1 NX5	5 Jan 2006	76.50	−170.00	54	6	0.17	0.43	0.26	21.2	1.5	81.0
CORSACS-1 NX5	5 Jan 2006	76.50	−170.00	54	16	0.14	0.40	0.27	22.5	1.6	82.2
CORSACS-1 NX5	5 Jan 2006	76.50	−170.00	54	36	0.12	0.47	0.36	24.1	1.8	81.9
CORSACS-1 NX5	5 Jan 2006	76.50	−170.00	54	56	0.13	0.49	0.36	26.3	2.0	82.8
CORSACS-1 NX5	5 Jan 2006	76.50	−170.00	54	76	0.15	0.94	0.78	28.2	2.0	84.5
CORSACS-1 NX5	5 Jan 2006	76.50	−170.00	54	96	0.13	0.79	0.66	28.8	2.1	83.8
CORSACS-1 NX5	5 Jan 2006	76.50	−170.00	54	146	0.18	1.70	1.52	30.0	2.2	85.8
CORSACS-1 NX5	5 Jan 2006	76.50	−170.00	54	196	0.29	2.81	2.53	30.7	2.2	87.4
CORSACS-1 NX5	5 Jan 2006	76.50	−170.00	54	296	0.30	4.90	4.59	30.7	2.2	87.3
CORSACS-1 NX6	7 Jan 2006	76.00	−176.62	31	6	0.22	0.28	0.06	20.6	1.4	71.2
CORSACS-1 NX6	7 Jan 2006	76.00	−176.62	31	16	0.10	0.31	0.21	20.5	1.5	71.1
CORSACS-1 NX6	7 Jan 2006	76.00	−176.62	31	36	0.11	0.64	0.54	27.7	2.0	82.3
CORSACS-1 NX6	7 Jan 2006	76.00	−176.62	31	56	0.13	0.96	0.83	28.8	2.0	82.5
CORSACS-1 NX6	7 Jan 2006	76.00	−176.62	31	76	0.15	1.30	1.16	28.1	2.1	82.9
CORSACS-1 NX6	7 Jan 2006	76.00	−176.62	31	96	0.24	6.41	6.16	31.4	2.3	90.0
CORSACS-1 NX6	7 Jan 2006	76.00	−176.62	31	146	0.16	2.83	2.68	30.1	2.2	89.5
CORSACS-1 NX6	7 Jan 2006	76.00	−176.62	31	196	0.15	1.71	1.57	29.4	2.1	91.3
CORSACS-1 NX6	7 Jan 2006	76.00	−176.62	31	296	0.20	3.33	3.13	31.2	2.2	84.7
CORSACS-1 NX7	9 Jan 2006	76.00	170.98	46	6	0.22	0.37	0.15	18.0	1.1	58.4
CORSACS-1 NX7	9 Jan 2006	76.00	170.98	46	16	0.07	0.41	0.34	18.0	1.1	58.7
CORSACS-1 NX7	9 Jan 2006	76.00	170.98	46	36	0.07	0.36	0.30	17.9	1.2	58.7
CORSACS-1 NX7	9 Jan 2006	76.00	170.98	46	56	0.08	0.49	0.42	17.6	1.2	62.8
CORSACS-1 NX7	9 Jan 2006	76.00	170.98	46	76	0.12	0.81	0.69	26.9	2.1	77.6
CORSACS-1 NX7	9 Jan 2006	76.00	170.98	46	96	0.09	1.45	1.37	27.6	2.1	80.3
CORSACS-1 NX7	9 Jan 2006	76.00	170.98	46	146	0.14	3.10	2.96	30.8	2.2	87.5
CORSACS-1 NX7	9 Jan 2006	76.00	170.98	46	196	0.15	2.90	2.76	30.9	2.3	81.9
CORSACS-1 NX7	9 Jan 2006	76.00	170.98	46	296	0.20	7.45	7.25	31.1	2.3	81.8
CORSACS-1 NX8	12 Jan 2006	77.50	−175.75	31	6	0.17	0.62	0.45	18.2	1.3	68.0
CORSACS-1 NX8	12 Jan 2006	77.50	−175.75	31	16	0.09	0.25	0.17	16.5	1.4	68.5
CORSACS-1 NX8	12 Jan 2006	77.50	−175.75	31	36	0.07	0.29	0.22	23.9	2.1	79.1
CORSACS-1 NX8	12 Jan 2006	77.50	−175.75	31	56	0.08	0.42	0.35	29.2	2.1	79.9
CORSACS-1 NX8	12 Jan 2006	77.50	−175.75	31	76	0.13	0.79	0.66	29.1	2.3	86.6
CORSACS-1 NX8	12 Jan 2006	77.50	−175.75	31	96	0.10	0.97	0.87	28.7	2.3	81.8
CORSACS-1 NX8	12 Jan 2006	77.50	−175.75	31	146	0.15	1.65	1.50	30.0	2.3	83.5
CORSACS-1 NX8	12 Jan 2006	77.50	−175.75	31	196	0.19	2.69	2.50	31.0	2.4	85.5
CORSACS-1 NX8	12 Jan 2006	77.50	−175.75	31	296	0.24	5.32	5.08	30.2	2.3	90.2
CORSACS-1 NX9	14 Jan 2006	78.65	−164.71	13	6	0.16	1.71	1.55	21.3	1.6	87.3

Table 1. (continued)

Station Name	Sampling Date	Latitude (°S)	Longitude (°E)	MLD[b] (m)	Depth (m)	dFe (nM)	TDFe (nM)	ALPFe[c] (nM)	N + N (μM)	DIP (μM)	Si (μM)
CORSACS-1 NX9	14 Jan 2006	78.65	−164.71	13	16	0.13	1.81	1.68	21.7	1.6	87.5
CORSACS-1 NX9	14 Jan 2006	78.65	−164.71	13	36	0.15	1.47	1.32	23.1	1.7	88.1
CORSACS-1 NX9	14 Jan 2006	78.65	−164.71	13	56	0.13	1.50	1.38	24.1	1.8	82.3
CORSACS-1 NX9	14 Jan 2006	78.65	−164.71	13	76	0.21	2.00	1.79	24.8	1.9	89.9
CORSACS-1 NX9	14 Jan 2006	78.65	−164.71	13	96	0.21	1.89	1.69	25.3	1.8	90.6
CORSACS-1 NX9	14 Jan 2006	78.65	−164.71	13	146	0.33	10.79	10.46	26.3	1.9	91.1
CORSACS-1 NX9	14 Jan 2006	78.65	−164.71	13	196	0.19	1.90	1.71	27.8	2.0	83.3
CORSACS-1 NX9	14 Jan 2006	78.65	−164.71	13	296	0.11	2.43	2.32	29.6	2.1	88.4
CORSACS-1 NX10	19 Jan 2006	75.00	164.99	29	6	0.28	1.10	0.82	20.8	1.3	62.1
CORSACS-1 NX10	19 Jan 2006	75.00	164.99	29	16	0.18	1.11	0.93	29.2	1.2	61.6
CORSACS-1 NX10	19 Jan 2006	75.00	164.99	29	36	0.19	1.02	0.83	23.6	1.7	67.4
CORSACS-1 NX10	19 Jan 2006	75.00	164.99	29	56	0.19	1.26	1.07	28.1	2.2	76.1
CORSACS-1 NX10	19 Jan 2006	75.00	164.99	29	76	0.30	1.64	1.34	28.2	2.2	75.5
CORSACS-1 NX10	19 Jan 2006	75.00	164.99	29	96	0.35	1.74	1.39	28.4	2.3	74.9
CORSACS-1 NX10	19 Jan 2006	75.00	164.99	29	146	0.40	1.92	1.52	28.3	2.2	74.7
CORSACS-1 NX10	19 Jan 2006	75.00	164.99	29	196	0.28	1.68	1.40	26.8	2.1	69.0
CORSACS-1 NX10	19 Jan 2006	75.00	164.99	29	296	0.34	1.76	1.42	27.8	2.2	73.1
CORSACS-1 NX10	19 Jan 2006	75.00	164.99	29	496	0.69	ND	ND	35.0	2.0	78.4
CORSACS-1 NX10	19 Jan 2006	75.00	164.99	29	596	0.64	ND	ND	34.0	2.0	80.3
CORSACS-1 NX10	19 Jan 2006	75.00	164.99	29	696	0.68	ND	ND	34.1	2.0	77.8
CORSACS-1 NX10	19 Jan 2006	75.00	164.99	29	796	0.64	ND	ND	33.9	2.0	77.6
CORSACS-1 NX11	21 Jan 2006	75.00	171.43	43	6	0.27	0.35	0.08	19.4	1.2	56.1
CORSACS-1 NX11	21 Jan 2006	75.00	171.43	43	16	0.08	0.21	0.13	19.4	1.2	55.6
CORSACS-1 NX11	21 Jan 2006	75.00	171.43	43	36	0.08	0.28	0.19	19.5	1.3	56.2
CORSACS-1 NX11	21 Jan 2006	75.00	171.43	43	56	0.09	0.41	0.33	26.2	2.1	77.0
CORSACS-1 NX11	21 Jan 2006	75.00	171.43	43	76	0.12	0.70	0.58	29.1	2.3	81.5
CORSACS-1 NX11	21 Jan 2006	75.00	171.43	43	96	0.20	1.97	1.77	30.9	2.3	85.5
CORSACS-1 NX11	21 Jan 2006	75.00	171.43	43	146	0.18	3.03	2.85	29.8	2.6	81.7
CORSACS-1 NX11	21 Jan 2006	75.00	171.43	43	196	0.21	3.55	3.34	30.5	2.3	83.5
CORSACS-1 NX11	21 Jan 2006	75.00	171.43	43	296	0.33	3.74	3.41	30.7	2.3	82.3
CORSACS-1 NX11	21 Jan 2006	75.00	171.43	43	396	0.42	ND	ND	30.7	2.4	87.3
CORSACS-1 NX11	21 Jan 2006	75.00	171.43	43	496	1.31	ND	ND	30.3	2.3	83.9
CORSACS-2 NX12	8 Nov 2006	65.21	−174.73	27	6	0.15	0.22	0.08	30.6	2.2	64.0
CORSACS-2 NX12	8 Nov 2006	65.21	−174.73	27	16	0.08	0.18	0.11	30.6	2.2	64.2
CORSACS-2 NX12	8 Nov 2006	65.21	−174.73	27	36	0.07	0.19	0.12	30.7	2.2	68.8
CORSACS-2 NX12	8 Nov 2006	65.21	−174.73	27	56	0.06	0.20	0.14	30.8	2.2	63.7
CORSACS-2 NX12	8 Nov 2006	65.21	−174.73	27	76	0.10	0.19	0.08	31.0	2.3	64.0
CORSACS-2 NX12	8 Nov 2006	65.21	−174.73	27	96	0.08	0.29	0.21	31.2	2.2	66.1
CORSACS-2 NX12	8 Nov 2006	65.21	−174.73	27	146	0.18	0.34	0.16	34.6	2.5	78.4
CORSACS-2 NX12	8 Nov 2006	65.21	−174.73	27	196	0.21	0.34	0.13	34.2	2.4	86.1
CORSACS-2 NX12	8 Nov 2006	65.21	−174.73	27	296	0.27	0.39	0.12	33.6	2.3	88.1
CORSACS-2 NX12	8 Nov 2006	65.21	−174.73	27	600	0.47	ND	ND	33.0	2.3	94.0
CORSACS-2 NX12	8 Nov 2006	65.21	−174.73	27	900	0.45	ND	ND	32.6	2.3	102.9
CORSACS-2 NX12	8 Nov 2006	65.21	−174.73	27	965	0.34	ND	ND	32.6	2.3	104.9
CORSACS-2 NX12	8 Nov 2006	65.21	−174.73	27	1265	0.38	ND	ND	32.9	2.3	104.9
CORSACS-2 NX13	16 Nov 2006	76.05	171.39	23	6	0.12	1.07	0.95	25.3	1.9	82.0
CORSACS-2 NX13	16 Nov 2006	76.05	171.39	23	16	0.07	1.33	1.26	27.7	2.1	81.9
CORSACS-2 NX13	16 Nov 2006	76.05	171.39	23	36	0.23	3.18	2.95	30.7	2.3	83.1
CORSACS-2 NX13	16 Nov 2006	76.05	171.39	23	56	0.21	3.24	3.04	30.5	2.3	81.7
CORSACS-2 NX13	16 Nov 2006	76.05	171.39	23	76	0.13	1.30	1.17	30.1	2.3	80.8
CORSACS-2 NX13	16 Nov 2006	76.05	171.39	23	96	0.19	2.16	1.97	31.1	2.3	82.2
CORSACS-2 NX13	16 Nov 2006	76.05	171.39	23	146	0.18	2.13	1.95	31.6	2.3	83.0
CORSACS-2 NX13	16 Nov 2006	76.05	171.39	23	196	0.17	1.66	1.49	31.1	2.3	84.1
CORSACS-2 NX13	16 Nov 2006	76.05	171.39	23	296	0.23	2.46	2.23	31.0	2.3	83.1
CORSACS-2 NX13	16 Nov 2006	76.05	171.39	23	400	0.30	10.92	10.61	31.1	2.4	83.5
CORSACS-2 NX13	16 Nov 2006	76.05	171.39	23	500	0.45	13.88	13.43	30.9	2.3	82.1
CORSACS-2 NX14	18 Nov 2006	75.93	178.36	131	6	0.10	0.55	0.45	27.7	2.2	73.4
CORSACS-2 NX14	18 Nov 2006	75.93	178.36	131	16	0.05	0.54	0.49	27.5	2.3	72.8
CORSACS-2 NX14	18 Nov 2006	75.93	178.36	131	36	0.06	0.54	0.48	27.5	2.2	75.9
CORSACS-2 NX14	18 Nov 2006	75.93	178.36	131	56	0.05	0.58	0.53	28.2	2.3	77.7
CORSACS-2 NX14	18 Nov 2006	75.93	178.36	131	76	0.07	0.62	0.55	28.8	2.3	79.8
CORSACS-2 NX14	18 Nov 2006	75.93	178.36	131	96	0.06	0.57	0.51	29.1	2.3	79.0
CORSACS-2 NX14	18 Nov 2006	75.93	178.36	131	146	0.12	1.13	1.01	29.5	2.4	81.2
CORSACS-2 NX14	18 Nov 2006	75.93	178.36	131	196	0.16	1.86	1.70	29.9	2.4	82.4
CORSACS-2 NX14	18 Nov 2006	75.93	178.36	131	296	0.19	1.62	1.43	30.1	2.5	82.6
CORSACS-2 NX14	18 Nov 2006	75.93	178.36	131	375	0.30	0.31	0.02	29.7	2.5	79.6
CORSACS-2 NX14	18 Nov 2006	75.93	178.36	131	450	0.37	0.41	0.04	29.7	2.5	79.0
CORSACS-2 NX15	20 Nov 2006	76.94	173.96	N/A	6	0.09	1.95	1.87	29.8	2.0	86.3
CORSACS-2 NX15	20 Nov 2006	76.94	173.96	N/A	16	0.11	1.99	1.88	29.5	2.0	86.0
CORSACS-2 NX15	20 Nov 2006	76.94	173.96	N/A	36	0.08	1.95	1.87	29.0	2.0	84.1
CORSACS-2 NX15	20 Nov 2006	76.94	173.96	N/A	56	0.08	2.00	1.93	28.8	1.9	82.8

Table 1. (continued)

Station Name	Sampling Date	Latitude (°S)	Longitude (°E)	MLD[b] (m)	Depth (m)	dFe (nM)	TDFe (nM)	ALPFe[c] (nM)	N + N (μM)	DIP (μM)	Si (μM)
CORSACS-2 NX15	20 Nov 2006	76.94	173.96	N/A	76	0.09	2.12	2.03	28.8	1.9	82.9
CORSACS-2 NX15	20 Nov 2006	76.94	173.96	N/A	96	0.09	2.30	2.21	29.0	2.0	82.8
CORSACS-2 NX15	20 Nov 2006	76.94	173.96	N/A	146	0.16	3.54	3.39	31.3	2.1	87.0
CORSACS-2 NX15	20 Nov 2006	76.94	173.96	N/A	196	0.14	1.28	1.13	31.5	2.1	84.0
CORSACS-2 NX15	20 Nov 2006	76.94	173.96	N/A	296	0.20	3.05	2.85	31.1	2.1	82.1
CORSACS-2 NX15	20 Nov 2006	76.94	173.96	N/A	375	0.22	0.44	0.22	30.9	2.1	84.4
CORSACS-2 NX16	24 Nov 2006	76.50	169.99	80	6	0.12	1.38	1.26	25.6	1.8	82.5
CORSACS-2 NX16	24 Nov 2006	76.50	169.99	80	16	0.08	1.47	1.39	25.8	1.9	82.2
CORSACS-2 NX16	24 Nov 2006	76.50	169.99	80	56	0.10	1.40	1.30	25.7	1.8	81.2
CORSACS-2 NX16	24 Nov 2006	76.50	169.99	80	76	0.04	1.75	1.70	27.0	2.1	81.1
CORSACS-2 NX16	24 Nov 2006	76.50	169.99	80	96	0.16	3.57	3.41	30.5	2.3	81.1
CORSACS-2 NX16	24 Nov 2006	76.50	169.99	80	146	0.19	2.47	2.29	30.4	2.4	80.9
CORSACS-2 NX16	24 Nov 2006	76.50	169.99	80	196	0.15	2.24	2.09	30.4	2.2	82.2
CORSACS-2 NX16	24 Nov 2006	76.50	169.99	80	296	0.20	4.96	4.76	30.9	2.2	77.0
CORSACS-2 NX16	24 Nov 2006	76.50	169.99	80	400	0.27	3.86	3.59	30.6	2.2	77.1
CORSACS-2 NX16	24 Nov 2006	76.50	169.99	80	500	0.33	8.16	7.83	30.5	2.3	81.2
CORSACS-2 NX17	26 Nov 2006	76.50	178.55	70	6	0.23	1.05	0.82	25.9	1.8	81.0
CORSACS-2 NX17	26 Nov 2006	76.50	178.55	70	16	0.09	0.60	0.51	28.0	2.0	79.2
CORSACS-2 NX17	26 Nov 2006	76.50	178.55	70	36	0.06	0.76	0.69	26.7	1.8	81.3
CORSACS-2 NX17	26 Nov 2006	76.50	178.55	70	56	0.07	0.66	0.59	27.1	1.9	80.9
CORSACS-2 NX17	26 Nov 2006	76.50	178.55	70	76	0.09	0.83	0.73	28.6	2.0	80.6
CORSACS-2 NX17	26 Nov 2006	76.50	178.55	70	96	0.05	0.85	0.79	28.8	2.2	79.9
CORSACS-2 NX17	26 Nov 2006	76.50	178.55	70	146	0.07	0.84	0.77	30.2	2.1	81.0
CORSACS-2 NX17	26 Nov 2006	76.50	178.55	70	196	0.17	1.73	1.56	31.0	2.1	81.9
CORSACS-2 NX17	26 Nov 2006	76.50	178.55	70	246	0.33	18.98	18.65	31.1	2.1	82.0
CORSACS-2 NX18	28 Nov 2006	77.76	178.49	156	6	0.05	1.25	1.19	24.9	2.0	83.1
CORSACS-2 NX18	28 Nov 2006	77.76	178.49	156	16	0.04	1.06	1.01	24.9	2.0	82.8
CORSACS-2 NX18	28 Nov 2006	77.76	178.49	156	36	0.05	1.28	1.24	27.2	2.2	84.4
CORSACS-2 NX18	28 Nov 2006	77.76	178.49	156	56	0.05	1.16	1.11	28.4	2.2	84.6
CORSACS-2 NX18	28 Nov 2006	77.76	178.49	156	76	0.06	1.77	1.71	29.9	2.4	83.4
CORSACS-2 NX18	28 Nov 2006	77.76	178.49	156	96	0.05	1.98	1.94	29.6	2.3	83.9
CORSACS-2 NX18	28 Nov 2006	77.76	178.49	156	146	0.06	1.70	1.64	29.8	2.4	84.6
CORSACS-2 NX18	28 Nov 2006	77.76	178.49	156	196	0.11	2.37	2.26	30.5	2.4	83.3
CORSACS-2 NX18	28 Nov 2006	77.76	178.49	156	296	0.10	1.71	1.62	30.6	2.4	84.3
CORSACS-2 NX18	28 Nov 2006	77.76	178.49	156	400	0.21	2.58	2.37	31.1	2.5	81.4
CORSACS-2 NX18	28 Nov 2006	77.76	178.49	156	500	0.25	2.85	2.60	31.4	2.5	80.5
CORSACS-2 NX18	28 Nov 2006	77.76	178.49	156	600	0.34	24.52	24.18	31.6	2.5	83.5
CORSACS-2 NX18	28 Nov 2006	77.76	178.49	156	700	0.43	68.40	67.98	31.5	2.5	81.6
CORSACS-2 NX19	30 Nov 2006	76.50	174.28	123	6	0.08	0.70	0.62	25.6	1.6	75.7
CORSACS-2 NX19	30 Nov 2006	76.50	174.28	123	16	0.04	0.68	0.65	27.0	1.8	79.2
CORSACS-2 NX19	30 Nov 2006	76.50	174.28	123	36	0.06	1.07	1.01	29.9	1.8	77.3
CORSACS-2 NX19	30 Nov 2006	76.50	174.28	123	56	0.10	1.25	1.15	30.5	2.1	78.2
CORSACS-2 NX19	30 Nov 2006	76.50	174.28	123	76	0.07	1.17	1.10	29.5	2.0	78.8
CORSACS-2 NX19	30 Nov 2006	76.50	174.28	123	96	0.09	1.22	1.14	30.0	2.0	78.3
CORSACS-2 NX19	30 Nov 2006	76.50	174.28	123	146	0.11	1.84	1.73	30.9	2.1	81.7
CORSACS-2 NX19	30 Nov 2006	76.50	174.28	123	196	0.12	2.21	2.09	30.6	2.1	80.9
CORSACS-2 NX19	30 Nov 2006	76.50	174.28	123	296	0.09	1.12	1.03	30.3	2.1	80.1
CORSACS-2 NX19	30 Nov 2006	76.50	174.28	123	375	0.30	6.80	6.50	31.0	2.1	79.7
CORSACS-2 NX19	30 Nov 2006	76.50	174.28	123	475	0.43	16.66	16.23	31.2	2.1	79.4
CORSACS-2 NX20	3 Dec 2006	76.50	−180.00	11	6	0.04	0.40	0.37	24.2	1.7	79.9
CORSACS-2 NX20	3 Dec 2006	76.50	−180.00	11	16	0.06	0.47	0.41	26.6	2.0	77.8
CORSACS-2 NX20	3 Dec 2006	76.50	−180.00	11	36	0.05	0.92	0.86	25.3	2.0	82.7
CORSACS-2 NX20	3 Dec 2006	76.50	−180.00	11	56	0.05	0.81	0.76	27.5	2.1	78.7
CORSACS-2 NX20	3 Dec 2006	76.50	−180.00	11	76	0.06	0.75	0.69	28.3	2.2	78.7
CORSACS-2 NX20	3 Dec 2006	76.50	−180.00	11	96	0.05	0.86	0.81	28.7	2.2	79.3
CORSACS-2 NX20	3 Dec 2006	76.50	−180.00	11	146	0.06	0.91	0.85	30.4	2.3	80.0
CORSACS-2 NX20	3 Dec 2006	76.50	−180.00	11	196	0.11	2.31	2.20	30.6	2.3	79.9
CORSACS-2 NX20 (0.2 μm)[d]	3 Dec 2006	76.50	−180.00	11	296	0.32	12.08	11.76	31.0	2.3	80.3
CORSACS-2 NX20 (0.4 μm)[d]	3 Dec 2006	76.50	−180.00	11	296	0.34	ND	ND	ND	ND	ND

[a]ND, not determined.
[b]Mixed layer depth determined based on $\Delta\sigma_t = 0.05$.
[c]ALPFe = TDFe − dFe.
[d]For comparison of dFe measured in water sample filtered using 0.2 μm pore Acropak capsule filter (0.2 μm) and 0.4 μm pore polycarbonate membrane filter (0.4 μm).

[22] Within this conceptual framework, the spring 2006 water column data reveal two puzzling features with regard to subsurface sources of dissolved iron. The first is at station NX14, in the trough between the Pennell and Ross banks, where deep samples were characterized by high dFe concentrations but no significant enrichment in TDFe or ALPFe (Figures 5d and 5h and Table 1). Similar features were observed in deep waters at station NX5 (Figures 5c and 5g),

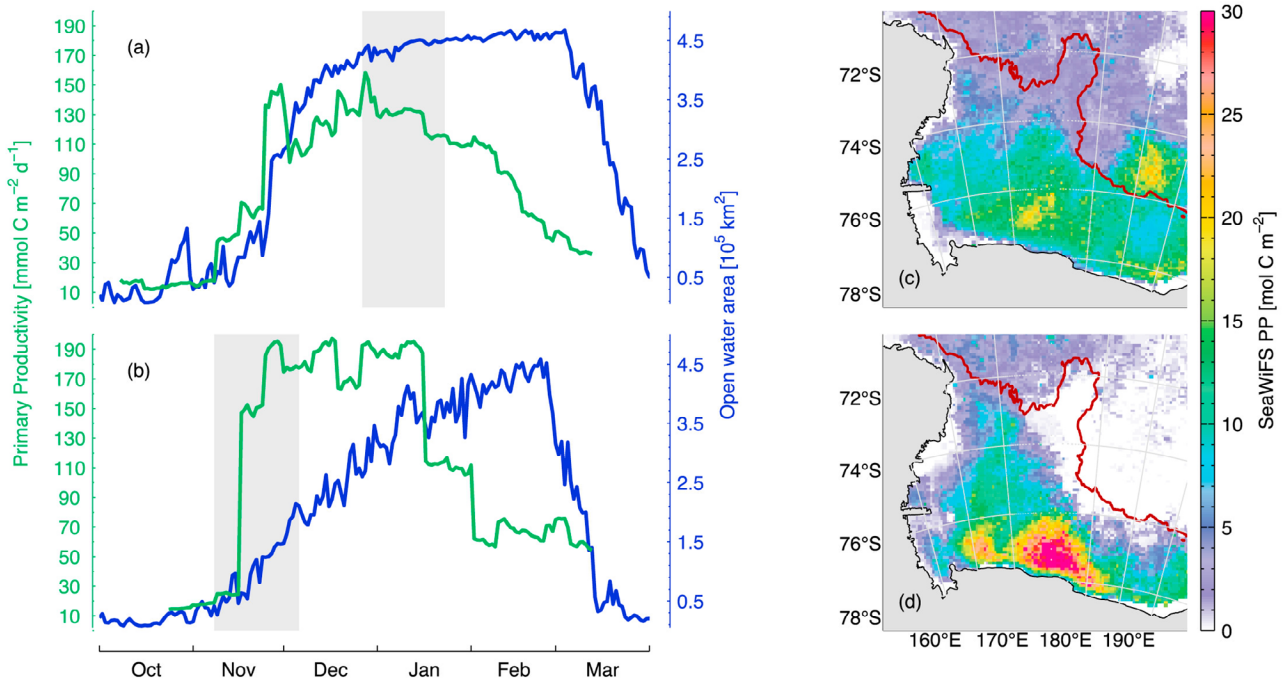

Figure 7. Time series of satellite-derived estimates of primary productivity and open-water (ice-free) area for Ross Sea Shelf over growing seasons in (a) 2005–2006 and (b) 2006–2007, using methods described by *Arrigo et al.* [2008a]; gray bars indicate the durations of CORSACS cruises. (c, d) Corresponding maps of the study region with seasonally integrated primary productivity estimates derived from SeaWiFS ocean-color data; red line indicates the 1000 m isobath.

where we have suggested that elevated dFe concentrations were associated with an intrusion of MCDW. However, our hydrographic data provide no evidence of MCDW intrusion near station NX14 (Figures 6d and 6h); thus the source of the deep dFe maximum at this location is not clear. A second perplexing feature is the bolus of relatively warm, oxygen-poor water observed at ~150–250 m depth near 175°E (Figures 6d and 6h), which likely reflects an intrusion of MCDW. As discussed above, we suggest that MCDW intrusions may carry elevated concentrations of dFe derived from the CDW. This hydrographic feature, however, shows no associated dFe enrichment (see Figure 5d, stations NX15 and NX19), implying that this MCDW intrusion did not carry elevated levels of dissolved iron. In this case, it is conceivable that dFe carried by this MCDW intrusion had already been lost by means of biological uptake and/or particle scavenging, given that low dFe concentrations extend to ~200 m depth along this zonal section; i.e., there is evidence of dFe depletion to depths of ~200 m along this section (see Figure 5d).

4. Discussion

[23] We propose that the low euphotic zone dFe concentrations in the Ross Sea polynya during spring 2006 reflect the rapid biological uptake of iron that occurred in the absence of significant iron inputs from melting sea ice. Along the quasi-zonal section shown in Figure 5d, which we sampled between 16 November and 3 December, phytoplankton biomass and production were relatively high: Measured chlorophyll concentrations in the upper 25 m were 1.8–6.0 μg L^{-1}, and column-integrated ^{14}C-based net primary productivity rates ranged from ~170 to 260 mmol C m^{-2} d^{-1} [*Long et al.*, 2011a]. This level of primary production does not appear to be unusual in the southern Ross Sea during spring, as similarly high values were measured in mid-November–early December 1994 [*Smith and Gordon*, 1997]. Furthermore, a Sea-viewing Wide Field-of-view Sensor (SeaWiFS)-based estimate of regional primary productivity [*Arrigo et al.*, 2008a] during the 2006–2007 growing season indicates that productivity in the polynya increased from ~20 mmol C m^{-2} d^{-1} to ~200 mmol C m^{-2} d^{-1} over a period of ~1 week in mid-November 2006 (Figure 7).

[24] It is difficult to estimate the corresponding biological drawdown in dFe, given the large uncertainty in the C/Fe assimilation ratio of the phytoplankton community, for which estimates range from ~10,000 to ~450,000 on a molar basis [*Twining et al.*, 2004; *Coale et al.*, 2005; *Tagliabue and Arrigo*, 2005]. However, we can make a rough estimate of the time period required for these levels of primary production to draw down surface dissolved iron from a likely winter reserve concentration of ~0.3 nM (based on measured subsurface dFe concentrations) to concentrations of around 0.1 nM, as observed during spring 2006. For this calculation we assume a sustained net community production of ~100 mmol C m^{-2} d^{-1}, which is based on measured net primary production rates of ~200 mmol C m^{-2} d^{-1} and an estimated *f* ratio of around 0.5 for our study region [*Asper and Smith*, 1999; *Long et al.*, 2011a]. Given algal C/Fe uptake ratios in the range of 10,000–450,000, this net community production could consume 0.2 nM dFe from the upper 100 m of the water column over a period of

2–90 days. Based on this estimate, there is clearly the potential for phytoplankton to effect a rapid drawdown in dissolved iron in surface waters of the Ross Sea polynya during the spring.

[25] Our results from the spring 2006 cruise are inconsistent with the conceptual model of gradual depletion of dFe in the Ross Sea polynya during the course of the growing season [e.g., *Sedwick et al.*, 2000; *Arrigo et al.*, 2003]. Rather, our field observations suggest that when irradiance-mixing conditions are favorable for net primary production, dFe can be drawn down to growth-limiting concentrations of ~0.1 nM over a period of less than a month, barring significant iron inputs to surface waters during that time. This scenario implies that iron availability may exert a first-order control on primary production rates in the Ross Sea polynya during both spring and summer, when the algal community is typically dominated by colonial *Phaeocystis antarctica* and by a mixed assemblage of *P. antarctica* and diatoms, respectively [*DiTullio and Smith*, 1996; *Smith et al.*, 2000; *Arrigo and van Dijken*, 2004; *Garrison et al.*, 2004]. This hypothesis is supported by the results of shipboard iron-addition experiments, which indicate that phytoplankton growth was limited by iron deficiency during both the summer 2005–2006 and spring 2006 cruises [*Bertrand et al.*, 2007, 2011; *Feng et al.*, 2010; *Rose et al.*, 2009]. Considered together, these findings imply that the typical seasonal succession of phytoplankton taxa in the southern Ross Sea does *not* reflect taxon-specific differences in cellular iron requirements, given that ambient dFe concentrations of less than ~0.1 nM are likely to limit the growth of both *P. antarctica* and diatoms [*Timmermans et al.*, 2001, 2004; *Garcia et al.*, 2009].

[26] Alternate interpretations of the CORSACS iron data are that spring 2006 represented an unusually early phytoplankton bloom in the southern Ross Sea, or that the winter reserve of dFe was unusually low at the start of the 2006–2007 growing season, either of which might be expected to result in the early depletion of dFe from surface waters of the polynya. However, these scenarios are not supported by other biological and biogeochemical data from the spring 2006 cruise [*Long et al.*, 2011a; *Tortell et al.*, 2011], which show that primary productivity, chlorophyll concentrations, nutrient drawdown, and pCO_2 were similar to values reported from previous spring cruises in the region [*Smith and Gordon*, 1997; *Bates et al.*, 1998; *Bender et al.*, 2000; *Gordon et al.*, 2000; *Smith et al.*, 2000]. Moreover, an unusually early spring bloom or a low initial inventory of dFe might be expected to result in truncation of the annual bloom, owing to the early depletion of dFe in the polynya. Contrary to this suggestion, the satellite-derived primary productivity estimates shown in Figure 7 [*Arrigo et al.*, 2008a] yield similar values for total primary production on the Ross Sea Shelf during the 2005–2006 (~31 Tg C) and 2006–2007 (~26 Tg C) growing seasons, with higher production in the central polynya during the 2006–2007 season (~20–25 mol C m^{-2} yr^{-1}) compared with the 2005–2006 season (~10–15 mol C m^{-2} yr^{-1}).

[27] Interestingly, the satellite-based productivity estimate for the 2006–2007 growing season (Figure 7b) suggests that the bulk of the annual primary production occurred *after* mid-November within the area surveyed during our cruise (~170°E–180°E, 76°S–78°S), even allowing for the inherent uncertainties in such satellite-derived productivity estimates. This begs the question as to the source of the iron that sustained phytoplankton production in the polynya from late November 2006 through late January 2007, given that we have documented likely growth-limiting dFe concentrations of ~0.1 nM in the euphotic zone of the polynya during the period mid-November–early December 2006 (Figures 2, 4, and 5d).

[28] Luxury uptake of dFe provides one possible source of iron to fuel primary production over the summer months, given that colonial *P. antarctica* are thought to accumulate iron in their extracellular mucus [*Schoemann et al.*, 2005] and that some pennate diatoms are known to use ferritin for intracellular iron storage [*Marchetti et al.*, 2009]. If we assume a minimum cellular iron requirement of ~2.2 μmol per mole of carbon (i.e., C/Fe = 450,000 mol mol^{-1}), then the drawdown of ~0.2 nM dFe over a 100 m deep surface mixed layer (=20 μmol Fe m^{-2}) could support a total seasonal new production of ~9 mol C m^{-2} yr^{-1}. This value is nearly half of the total production estimated for the central polynya during the 2006–2007 season (Figure 7b) and suggests that luxury uptake of Fe could support most of the estimated seasonal production in this region, assuming an *f* ratio (= new production/total net production) of ~0.5 [*Asper and Smith*, 1999; *Sweeney et al.*, 2000; *Long et al.*, 2011a]. However, *Coale et al.* [2005] have used seasonal changes in particulate Fe/Al ratios in the Ross Sea to estimate a net biological utilization of 450–633 μmol Fe m^{-2} along 76°30′S during the 1996–1997 growth season. These values are more than 20-fold higher than our estimate of biological dFe drawdown during spring and imply an effective algal C/Fe assimilation ratio that is more than an order of magnitude less than 450,000 mol mol^{-1}, given that satellite-derived estimates suggest a net primary production on the order of 10 mol C m^{-2} yr^{-1} in the Ross Sea polynya. Clearly, the much larger seasonal iron utilization estimated by *Coale et al.* [2005] would require a significant input of biologically available "new" iron to surface waters of the Ross Sea polynya during the growing season.

[29] We can suggest four likely sources of new dFe in the upper water column during the growing season. The first is the relatively large pool of particulate iron in surface waters over the inner shelf, where we estimate that ALPFe concentrations often exceed 0.5 nM (Table 1). In this respect, the inner-shelf surface waters contrast strongly with the deep-ocean station NX12, where near-surface ALPFe concentrations were only ~0.1 nM (Table 1). In surface waters of the polynya, this particulate iron is likely to be associated not only with biogenic material, from which dFe may be regenerated (thus "recycled" dFe), but also with inorganic phases (e.g., aluminosilicates, oxyhydroxides) and allochtonous organic particles derived from sea ice, nearshore sediments, and atmospheric deposition. These latter materials are potential sources of new iron, which may be rendered biologically available by means of dissolution, photoreduction, and/or biological processing in surface waters during the growing season [*Barbeau et al.,* 2001; *Boyd et al.*, 2005; *Boyd and Ellwood*, 2010]. It is interesting to note that our iron data from both cruises indicate elevated concentrations of ALPFe in surface waters over the inner shelf (Table 1),

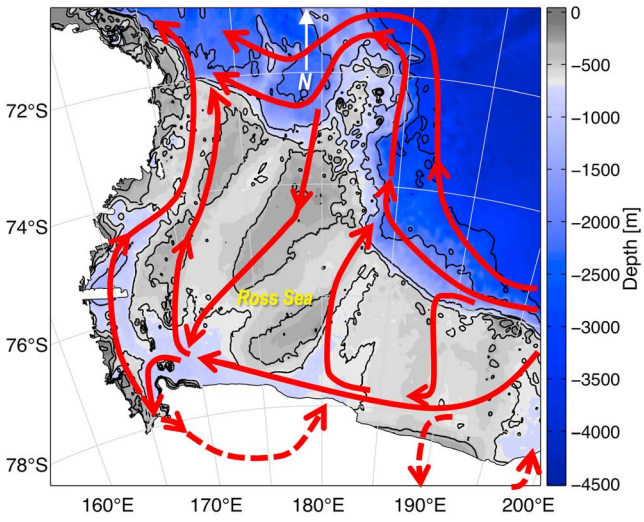

Figure 8. Schematic diagram of surface circulation in the Ross Sea, based on the works of *Locarnini* [1994], *Jacobs and Giulivi* [1998], *Dinniman et al.* [2003], and *Smith et al.* [2007].

where the satellite-derived estimates of seasonal primary production were highest (Figure 7). This perhaps reflects the role of particulate iron in fuelling this high primary production.

[30] A second potential source of new dFe to surface waters of the polynya during summer months is by means of vertical exchange with iron-rich deeper waters. Our summer 2005–2006 data show that dFe concentrations can reach ~0.3–0.5 nM at depths of 100–200 m in some areas of the polynya (Figures 3 and 5c). These dFe-enriched waters lie below the depth of the surface mixed layer during summer; however, mesoscale eddies and fronts, which can uplift isopycnal surfaces by tens to hundreds of meters, could facilitate the episodic injection of these iron-rich waters into the euphotic zone, in the same manner as has been suggested for macronutrients in the oligotrophic ocean [*McGillicuddy et al.*, 2003, 2007]. Although biogeochemical observations in the Ross Sea have largely been made over spatial and temporal scales that do not allow the resolution of such transient mesoscale features, the results of underway sampling have revealed significant variability at the mesoscale and submesoscale [*Hales and Takahashi*, 2004; *Tortell and Long*, 2009], as have satellite ocean-color images and numerical simulations of regional circulation [*Dinniman et al.*, 2003, 2011; *Reddy and Arrigo*, 2006]. One potential problem with vertical exchange as a mechanism to supply new iron during the summer is that this process would also introduce macronutrients to the euphotic zone, which would tend to counter the progressive drawdown in surface nutrients that is observed during the summer months [e.g., see *Smith et al.*, 2003]. However, it is difficult to evaluate this issue quantitatively, given the uncertainties in the algal assimilation of dFe relative to macronutrients and in the relative concentrations of dFe and macronutrients that may be supplied from subsurface waters.

[31] Horizontal advection provides a third possible mechanism to supply iron to surface waters of the polynya, by redistributing dFe that is released from melting sea ice on the margins of the polynya and/or from shallow benthic sources in the southwestern Ross Sea. In addition, any dFe that is introduced to surface waters in localized areas of enhanced vertical exchange (e.g., over shallow bottom features) may be further distributed to the polynya by means of lateral transport and mixing. Mean surface circulation over the Ross Sea Shelf is generally toward the west and north (Figure 8), following the southwest limb of the Ross Sea gyre, although there is likely some smaller-scale transport to the east and south that occurs within this regional circulation pattern [*Assmann et al.*, 2003; *Dinniman et al.*, 2003; *Reddy and Arrigo*, 2006]. This lateral circulation provides the potential for the transport of iron-enriched waters into the central polynya from melting sea ice in the east and from sea ice and/or benthic iron sources in the south and west. *Reddy and Arrigo* [2006] have further argued that the intrusion of iron-poor surface waters from north of the shelf break restricts phytoplankton blooms to the southwestern Ross Sea, where there is a greater supply of biologically available iron. Mesoscale eddies may also provide an important mechanism for the horizontal transport of dFe into the polynya, in a manner similar to that described for the Haida, Sitka, and Yakutat eddies that transport dFe into surface waters of the central Gulf of Alaska [*Johnson et al.*, 2005; *Ladd et al.*, 2009].

[32] A fourth potential source of new iron to the Ross Sea is from the deposition of aerosol iron, some fraction of which will dissolve in surface waters of the polynya, as documented in other oceanic regions [e.g., *Sedwick et al.*, 2005; *Bonnet and Guieu*, 2006]. Much of the iron-bearing dust deposited during the winter will accumulate in snow on the sea ice and then enter the water column when the sea ice melts in spring and summer [*Sedwick and DiTullio*, 1997; *Edwards and Sedwick*, 2001]. In the context of iron inputs to the ice-free waters of the polynya during summer, the dust released from sea ice could arguably be considered as a potential input by means of horizontal advection, along with iron that is contained in the sea ice itself [*Lannuzel et al.*, 2007; *Lancelot et al.*, 2009]. However, some aerosol iron will also be deposited to the polynya during the growing season, providing a direct input of dFe to these surface waters. In either case, the primary production that is fuelled by aeolian iron input is likely to be small, based on regional-scale estimates of mineral dust deposition to the Southern Ocean [*Duce and Tindale*, 1991; *Edwards and Sedwick*, 2001; *Wagener et al.*, 2008; *Lancelot et al.*, 2009]. For example, an estimated aeolian iron flux to the Ross Sea of ~2 μmol m^{-2} yr^{-1} [*Edwards and Sedwick*, 2001] could support less than 1 mol C m^{-2} yr^{-1} of new production, assuming a relatively high algal C/Fe assimilation ratio of 450,000 mol mol^{-1} [*Tagliabue and Arrigo*, 2005]. It is of course possible that the southern Ross Sea might receive larger, episodic inputs of Fe-bearing dust carried by katabatic winds from local sources, such as the McMurdo Dry Valleys and Ross Island, although so far there are no data that document such inputs or their potential to add dissolved iron to the polynya.

[33] Our present data set does not allow us to confidently exclude any of these four potential sources of new iron to the Ross Sea polynya during summer, given the short duration of our cruise observations relative to the longer period over which these iron inputs might occur (see Figure 7). We suggest that some combination of targeted process studies

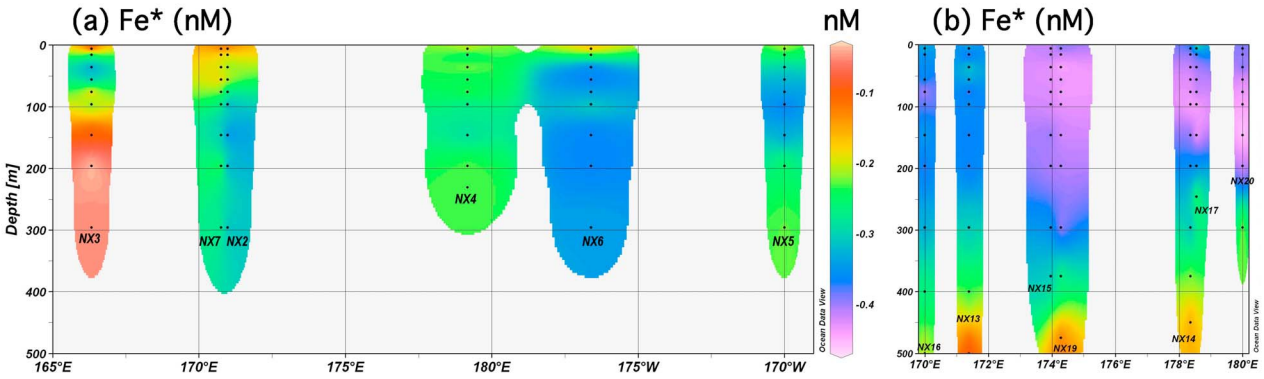

Figure 9. Quasi-zonal sections of Fe* (see text for definition) for (a) summer 2005–2006 and (b) spring 2006 cruises. Calculated using data from stations at locations shown in Figures 5a and 5b.

and seasonal-scale time series observations would be required in order to critically evaluate these proposed iron sources. To this end, there is a clear need for information regarding (1) the reactivity and biological availability of particulate Fe in the Ross Sea, (2) the potential for lateral and vertical transport of dFe into the polynya during summer, (3) the effective iron/macronutrient assimilation ratios of native phytoplankton, and (4) the magnitude and variability of aerosol iron deposition in our study region. The results of our study highlight the need to better understand the role of MCDW in delivering iron to subsurface waters, which may provide a source of dissolved iron to the euphotic zone. Also of potential importance in this regard are subsurface intrusions of ISW from the Ross Ice Shelf [*Jacobs et al.*, 1970; *Smethie and Jacobs*, 2005], which might be expected to carry iron derived from glacial ice and subglacial debris [*Fitzwater et al.*, 2000; *Sedwick et al.*, 2000]. Hydrographic data from the spring 2006 cruise suggest an intrusion of ISW near the 180° meridian at a depth of ~400 m (Figures 6d and 6f), although no samples for iron analysis were collected within this depth range. Hence the targeted sampling of both MCDW and ISW for iron analysis is an obvious direction for future research in the Ross Sea.

[34] Despite the elevated concentrations of dFe in subsurface waters of the Ross Sea, a comparison with corresponding macronutrient concentrations suggests that there is an insufficient inventory of dFe in the water column to support complete biological utilization of macronutrients if vertical resupply constitutes the major source of dFe to the euphotic zone. Here a quantitative assessment is provided by the diagnostic tracer Fe* [*Parekh et al.*, 2005], which estimates the concentration of dFe present in excess of that required to consume all dissolved macronutrients in phytoplankton biomass. Here we calculate Fe* based on nitrate plus nitrite (rather than phosphate, as was used by *Parekh et al.*, [2005]): $Fe^* = [dFe] - R_{Fe}[N + N]$, where [dFe] and [N + N] are the concentrations of dFe (nM) and nitrate plus nitrite (μM), respectively, and R_{Fe} is the Fe/N assimilation ratio for phytoplankton in nmol μmol^{-1}. Choosing a relatively low Fe/C assimilation ratio of 2.22 μmol mol^{-1} (i.e., C/Fe = 450,000 mol mol^{-1} [*Tagliabue and Arrigo*, 2005]) and a C/N assimilation ratio of 7.81 mol mol^{-1} [*Arrigo et al.*, 1999] for *Phaeocystis*-dominated waters yields an R_{Fe} value of 0.0174 nmol μmol^{-1}. Figure 9 shows quasi-zonal sections constructed from thus calculated Fe* values for stations between 76°S and 77°S. These Fe* values are generally less than zero for both the summer 2005–2006 and spring 2006 cruises, suggesting a general deficiency in dissolved iron relative to dissolved inorganic nitrogen in terms of the concentrations required to support phytoplankton growth.

[35] There is of course considerable uncertainty in the algal Fe/N assimilation ratio, with 2.22 μmol mol^{-1} representing a conservatively low estimate; i.e., a relatively high estimate for the C/Fe assimilation ratio [*Twining et al.*, 2004; *Coale et al.*, 2005, *Tagliabue and Arrigo*, 2005]. Choosing a higher Fe/N ratio, and hence a higher R_{Fe} value, will result in even larger negative values for Fe* (that is, a greater deficiency of dissolved iron relative to nitrogen) than the values shown in Figure 9. These calculations demonstrate the general propensity for iron limitation of primary production in the southern Ross Sea if dFe is primarily supplied by means of vertical exchange processes and underscore the potential importance of any new dFe that may be provided by other sources. In this context we note that a small number of stations sampled during the summer 2005–2006 cruise were unusual in showing a near-complete drawdown of nitrate and phosphate in surface waters [*Long et al.*, 2011a]. These stations were all located along the western edge of the study region, adjacent to sea ice, which may provide a source of new iron that allowed phytoplankton to consume more macronutrients in these waters.

5. Concluding Remarks

[36] The results from the CORSACS cruises suggest that surface waters in the Ross Sea polynya can become iron depleted during an early stage of the seasonal phytoplankton bloom. Thus the conceptual model of the southern Ross Sea as a region where dFe is gradually depleted during the growing season [e.g., *Sedwick et al.*, 2000] must be modified to allow that the polynya may become iron limited during spring, such that dFe availability regulates primary production during much of the period when there is sufficient light to sustain net phytoplankton growth. Moreover, the fact that field and satellite observations have documented a significant accumulation of phytoplankton biomass in the Ross Sea polynya during the summer months, despite low surface dFe concentrations, suggests that there is a significant

supply of "new" dFe to surface waters of the polynya over this period. This further implies that the supply of dFe to the euphotic zone during the growing season may exert a significant control on the magnitude of annual primary production in the Ross Sea polynya and hence on the magnitude of biological CO_2 uptake on the Ross Sea shelf.

[37] Given the potentially large CO_2 sink associated with primary production on the Ross Sea shelf [*Arrigo et al.*, 2008b] and the likely importance of iron in regulating this production, it is clearly of interest to better understand the processes that supply iron to these waters and the potential impacts of climatic variability and climate change on these processes. In the Ross Sea, future climate warming may be expected to eventually reduce seasonal sea ice cover while increasing vertical stratification and the input of glacial meltwaters [*Jacobs et al.*, 2002; *Sarmiento et al.*, 2004; *Boyd et al.*, 2008]. However, these changes may be tempered by an enhanced ventilation of the Southern Ocean as a result of an intensification and poleward shift in the westerly winds [*Le Quere et al.*, 2007; *Lenton et al.*, 2009]. Each of these climatic forcings may be expected to have an impact on the supply of iron to surface waters of the Ross Sea polynya, as well as the mean irradiance within these waters, which will in turn alter phytoplankton iron requirements [*Sunda and Huntsman*, 1997; *Boyd*, 2002; *Galbraith et al.*, 2010]. At present, the net result of these impacts cannot be reliably estimated, given our still-limited understanding of the sources, sinks, and cycling of iron on the Antarctic continental margins.

[38] **Acknowledgments.** We thank the members of the CORSACS science team, the officers and crew of RVIB *Nathaniel B. Palmer*, and the field support personnel of the Raytheon Polar Services Company for their contributions to this research. We are grateful to Ken Bruland and Geoffrey Smith for providing the towfish underway sampling system; to Angela Milne and Juliette Tria for assistance with the shipboard sampling; and to Mike Dinninan for helpful discussions. We also thank three anonymous reviewers and the editors for their numerous comments and suggestions, which have greatly improved the paper. This research was supported by U.S. National Science Foundation awards OPP-0338164 to PNS, OPP-0338350 to RBD, OPP-0440840 to MAS, OPP-0338157 to WOS, and OPP-0338097 to GRD.

References

Amante, C., and B. W. Eakins (2008), *ETOPO1 1 Arc-Minute Global Relief Model: Procedures, Data Sources and Analysis*, *NOAA Tech. Memo. 24*, Natl. Geophys. Data Cent., Boulder, Colo.

Arrigo, K. R., and G. L. van Dijken (2004), Annual changes in sea ice, chlorophyll *a*, and primary production in the Ross Sea, Antarctica, *Deep Sea Res., Part II*, *51*, 117–138, doi:10.1016/j.dsr2.2003.04.003.

Arrigo, K. R., D. H. Robinson, D. L. Worthen, R. B. Dunbar, G. R. DiTullio, M. L. VanWoert, and M. P. Lizotte (1999), Phytoplankton community structure and the drawdown of nutrients and CO_2 in the Southern Ocean, *Science*, *283*, 365–367, doi:10.1126/science.283.5400.365.

Arrigo, K. R., D. L. Worthen, and D. H. Robinson (2003), A coupled ocean-ecosystem model of the Ross Sea: 2. Iron regulation of phytoplankton taxonomic variability and primary production, *J. Geophys. Res.*, *108*(C7), 3231, doi:10.1029/2001JC000856.

Arrigo, K. R., G. L. van Dijken, and S. Bushinsky (2008a), Primary production in the Southern Ocean, 1997–2006, *J. Geophys. Res.*, *113*, C08004, doi:10.1029/2007JC004551.

Arrigo, K. R., G. van Dijken, and M. Long (2008b), Coastal Southern Ocean: A strong anthropogenic CO_2 sink, *Geophys. Res. Lett.*, *35*, L21602, doi:10.1029/2008GL035624.

Asper, V. L., and W. O. Smith Jr. (1999), Particle fluxes during austral spring and summer in the southern Ross Sea, Antarctica, *J. Geophys. Res.*, *104*(C3), 5345–5359, doi:10.1029/1998JC900067.

Assmann, K., H. H. Hellmer, and A. Beckmann (2003), Seasonal variation in circulation and water mass distribution on the Ross Sea continental shelf, *Antarct. Sci.*, *15*, 3–11, doi:10.1017/S0954102003001007.

Barbeau, K., E. L. Rue, K. W. Bruland, and A. Butler (2001), Photochemical cycling of iron in the surface ocean mediated by microbial iron (III)-binding ligands, *Nature*, *413*, 409–413, doi:10.1038/35096545.

Bates, N. R., D. A. Hansell, C. A. Carlson, and L. I. Gordon (1998), Distribution of CO_2 species, estimates of net community production, and air-sea CO_2 exchange in the Ross Sea polynya, *J. Geophys. Res.*, *103*(C2), 2883–2896, doi:10.1029/97JC02473.

Bender, M. L., M.-L. Dickson, and J. Orchardo (2000), Net and gross production in the Ross Sea as determined by incubation experiments and dissolved O_2 studies, *Deep Sea Res., Part II*, *47*, 3141–3158, doi:10.1016/S0967-0645(00)00062-X.

Bertrand, E. M., M. A. Saito, J. M. Rose, C. R. Riesselman, M. C. Lohan, A. E. Noble, P. A. Lee, and G. R. DiTullio (2007), Vitamin B_{12} and iron colimitation of phytoplankton growth in the Ross Sea, *Limnol. Oceanogr.*, *52*, 1079–1093, doi:10.4319/lo.2007.52.3.1079.

Bertrand, E. M., M. A. Saito, P. A. Lee, and G. R. DiTullio (2011), Iron limitation of springtime bacterial and phytoplankton populations in the Ross Sea: Interactive effects of iron and vitamin B_{12} nutrition, *Front. Aquat. Microbiol.*, *2*, 160, doi:10.3389/fmicb.2011.00160.

Bonnet, S., and C. Guieu (2006), Atmospheric forcing on the annual iron cycle in the western Mediterranean Sea: A 1-year survey, *J. Geophys. Res.*, *111*, C09010, doi:10.1029/2005JC003213.

Boyd, P. W. (2002), Environmental factors controlling phytoplankton processes in the Southern Ocean, *J. Phycol.*, *38*, 844–861, doi:10.1046/j.1529-8817.2002.t01-1-01203.x.

Boyd, P. W., and M. J. Ellwood (2010), The biogeochemical cycle of iron in the ocean, *Nat. Geosci.*, *3*, 675–682, doi:10.1038/ngeo964.

Boyd, P. W., et al. (2005), FeCycle: Attempting an iron biogeochemical budget from a mesoscale SF6 tracer experiment in unperturbed low iron waters, *Global Biogeochem. Cycles*, *19*, GB4S20, doi:10.1029/2005GB002494.

Boyd, P. W., S. C. Doney, R. Strzepek, J. Dusenberry, K. Lindsay, and I. Fung (2008), Climate-mediated changes to mixed-layer properties in the Southern Ocean: Assessing the phytoplankton response, *Biogeosciences*, *5*, 847–864, doi:10.5194/bg-5-847-2008.

Bruland, K. W., E. L. Rue, G. J. Smith, and G. R. DiTullio (2005), Iron, macronutrients and diatom blooms in the Peru upwelling regime: Brown and blue waters of Peru, *Mar. Chem.*, *93*, 81–103, doi:10.1016/j.marchem.2004.06.011.

Coale, K. H., X. Wang, S. J. Tanner, and K. S. Johnson (2003), Phytoplankton growth and biological response to iron and zinc addition in the Ross Sea and Antarctic Circumpolar Current along 170°W, *Deep Sea Res., Part II*, *50*, 635–653, doi:10.1016/S0967-0645(02)00588-X.

Coale, K. H., R. M. Gordon, and X. Wang (2005), The distribution and behavior of dissolved and particulate iron and zinc in the Ross Sea and Antarctic circumpolar current along 170°W, *Deep Sea Res., Part I*, *52*, 295–318, doi:10.1016/j.dsr.2004.09.008.

Dinniman, M. S., J. M. Klinck, and W. O. Smith (2003), Cross-shelf exchange in a model of Ross Sea circulation and biogeochemistry, *Deep Sea Res., Part II*, *50*, 3103–3120, doi:10.1016/j.dsr2.2003.07.011.

Dinniman, M. S., J. M. Klinck, and W. O. Smith (2011), A model study of circumpolar deep water on the west Antarctic Peninsula and Ross Sea continental shelves, *Deep Sea Res., Part II*, *58*, 1508–1523, doi:10.1016/j.dsr2.2010.11.013.

DiTullio, G. R., and W. O. Smith (1996), Spatial patterns in phytoplankton biomass and pigment distributions in the Ross Sea, *J. Geophys. Res.*, *101*(C8), 18,467–18,477, doi:10.1029/96JC00034.

DiTullio, G. R., J. M. Grebmeier, K. R. Arrigo, M. P. Lizotte, D. H. Robinson, A. R. Leventer, J. P. Barry, M. van Woert, and R. B. Dunbar (2000), Rapid and early export of *Phaeocystis antarctica* blooms in the Ross Sea, Antarctica, *Nature*, *404*, 595–598, doi:10.1038/35007061.

Duce, R., and N. W. Tindale (1991), Atmospheric transport of iron and its deposition in the ocean, *Limnol. Oceanogr.*, *36*, 1715–1726, doi:10.4319/lo.1991.36.8.1715.

Edwards, R., and P. Sedwick (2001), Iron in east Antarctic snow: Implications for atmospheric iron deposition and algal production in Antarctic waters, *Geophys. Res. Lett.*, *28*(20), 3907–3910, doi:10.1029/2001GL012867.

Feng, Y., et al. (2010), Interactive effects of iron, irradiance and CO_2 on Ross Sea phytoplankton, *Deep Sea Res., Part I*, *57*, 368–383, doi:10.1016/j.dsr.2009.10.013.

Fitzwater, S. E., K. S. Johnson, R. M. Gordon, K. H. Coale, and W. O. Smith (2000), Trace metal concentrations in the Ross Sea and their relationship with nutrients and growth, *Deep Sea Res., Part II*, *47*, 3159–3179, doi:10.1016/S0967-0645(00)00063-1.

Galbraith, E. D., A. Gnanadesikan, J. P. Dunne, and M. R. Hiscock (2010), Regional impacts of iron-light colimitation in a global biogeochemical model, *Biogeosciences*, *7*, 1043–1064, doi:10.5194/bg-7-1043-2010.

Garcia, N. S., P. N. Sedwick, and G. R. DiTullio (2009), Influence of irradiance and iron on the growth of colonial *Phaeocystis antarctica*:

Implications for seasonal bloom dynamics in the Ross Sea, Antarctica, *Aquat. Microb. Ecol.*, *57*, 203–220, doi:10.3354/ame01334.

Garrison, D. L., A. Gibson, H. Kunze, M. M. Gowing, C. L. Vickers, S. Mathot, and R. C. Bayreothers (2004), The Ross Sea Polynya Project: Diatom- and *Phaeocystis*-dominated phytoplankton assemblages in the Ross Sea, Antarctica 1994–1996, in *Biogeochemistry of the Ross Sea*, *Antarct. Res. Ser.*, vol. 78, edited by G. R. DiTullio and R. B. Dunbar, pp. 53–76, AGU, Washington, D. C.

Gordon, L. I., J. C. Jennings, A. A. Ross, and J. M. Krest (1993), A suggested protocol for flow automated analysis of seawater nutrients, in *Methods Manual WHPO 91–1*, World Ocean Circ. Exp. Hydrogr. Program Off., La Jolla, Calif.

Gordon, L. I., L. A. Codispoti, J. C. Jennings Jr., F. J. Millero, J. M. Morrison, and C. Sweeney (2000), Seasonal evolution of hydrographic properties in the Ross Sea, Antarctica, 1996–1997, *Deep Sea Res., Part II*, *47*, 3095–3117, doi:10.1016/S0967-0645(00)00060-6.

Grotti, M., F. Soggia, C. Ianni, and R. Frache (2005), Trace metals distributions in coastal sea ice of Terra Nova Bay, Ross Sea, Antarctica, *Antarct. Sci.*, *17*, 289–300, doi:10.1017/S0954102005002695.

Hales, B., and T. Takahashi (2004), High-resolution biogeochemical investigation of the Ross Sea, Antarctica, during the AESOPS (U. S. JGOFS) Program, *Global Biogeochem. Cycles*, *18*, GB3006, doi:10.1029/2003GB002165.

Hofmann, E. E., and J. M. Klinck (1998), Hydrography and circulation of the Antarctic continental shelf: 150°E eastward to the Greenwich Meridian, in *The Sea*, vol. 11, *The Global Coastal Ocean: Regional Studies and Synthesis*, edited by A. R. Robinson and K. H. Brink, pp. 997–1042, Harvard Univ. Press, Cambridge, Mass.

Jacobs, S. S., and C. F. Giulivi (1998), Interannual ocean and sea ice variability in the Ross Sea, *Antarct. Res. Ser.*, *75*, 135–150, doi:10.1029/AR075p0135.

Jacobs, S. S., A. F. Amos, and P. M. Bruchhausen (1970), Ross Sea oceanography and Antarctic bottom water formation, *Deep Sea Res., Part I*, *17*, 935–962.

Jacobs, S. S., C. F. Giulivi, and P. A. Mele (2002), Freshening of the Ross Sea during the late 20th century, *Science*, *297*, 386–389, doi:10.1126/science.1069574.

Johnson, K. S., R. M. Gordon, and K. H. Coale (1997), What controls dissolved iron concentrations in the world ocean?, *Mar. Chem.*, *57*, 137–161, doi:10.1016/S0304-4203(97)00043-1.

Johnson, K. S., et al. (2007), Developing standards for dissolved iron in seawater, *Eos Trans. AGU*, *88*, 131–132, doi:10.1029/2007EO110003.

Johnson, K. W., L. A. Miller, N. E. Sutherland, and C. S. Wong (2005), Iron transport by mesoscale Haida eddies in the Gulf of Alaska, *Deep Sea Res., Part II*, *52*, 933–953, doi:10.1016/j.dsr2.2004.08.017.

Ladd, C., W. R. Crawford, C. E. Harpold, W. K. Johnson, N. B. Kachel, P. J. Stabeno, and F. Whitney (2009), A synoptic survey of young mesoscale eddies in the Eastern Gulf of Alaska, *Deep Sea Res., Part II*, *56*, 2460–2473, doi:10.1016/j.dsr2.2009.02.007.

Lancelot, C., A. de Montety, H. Goosse, S. Becquevort, V. Schoemann, B. Pasquer, and M. Vancoppenolle (2009), Spatial distribution of the iron supply to phytoplankton in the Southern Ocean: A model study, *Biogeosciences*, *6*, 2861–2878, doi:10.5194/bg-6-2861-2009.

Lannuzel, D., V. Schoemann, J. de Jong, J.-L. Tison, and L. Chou (2007), Distribution and biogeochemical behavior of iron in the East Antarctic sea ice, *Mar. Chem.*, *106*, 18–32, doi:10.1016/j.marchem.2006.06.010.

Lenton, A., F. Codron, L. Bopp, N. Metzl, P. Cadule, A. Tagliabue, and J. Le Sommer (2009), Stratospheric ozone depletion reduces ocean carbon uptake and enhances ocean acidification, *Geophys. Res. Lett.*, *36*, L12606, doi:10.1029/2009GL038227.

Le Quere, C., et al. (2007), Saturation of the Southern Ocean CO_2 sink due to recent climate change, *Science*, *316*, 1735–1738, doi:10.1126/science.1136188.

Locarnini, R. A. (1994), Water masses and circulation in the Ross Gyre and environs, Ph.D. dissertation, 87 pp., Tex. A&M Univ., College Station, Tex.

Long, M. C., R. B. Dunbar, P. D. Tortell, W. O. Smith, D. A. Mucciarone, and G. R. DiTullio (2011a), Vertical structure, seasonal drawdown, and net community production in the Ross Sea, Antarctica, *J. Geophys. Res.*, *116*, C10029, doi:10.1029/2009JC005954.

Long, M. C., L. F. Thomas, and R. B. Dunbar (2011b), Control of phytoplankton bloom inception in the Ross Sea, Antarctica by Ekman restratification, *Global Biogeochem. Cycles*, doi:10.1029/2010GB003982, in press.

Marchetti, A., M. S. Parker, L. P. Moccia, E. O. Lin, A. L. Arrieta, F. Ribalet, M. E. P. Murphy, M. T. Maldonado, and E. V. Armbrust (2009), Ferritin is used for iron storage in bloom-forming marine pennate diatoms, *Nature*, *457*, 467–470, doi:10.1038/nature07539.

Marinov, I., A. Gnanadesikan, J. R. Toggweiler, and J. L. Sarmiento (2006), The Southern Ocean biogeochemical divide, *Nature*, *441*, 964–967, doi:10.1038/nature04883.

Markus, T., and B. A. Burns (1995), A method to estimate subpixel-scale coastal polynyas with satellite passive microwave data, *J. Geophys. Res.*, *100*(C3), 4473–4487, doi:10.1029/94JC02278.

Martin, J. H., S. E. Fitzwater, and R. M. Gordon (1990), Iron deficiency limits plankton growth in Antarctic waters, *Global Biogeochem. Cycles*, *4*, 5–12, doi:10.1029/GB004i001p00005.

Martin, J. H., R. M. Gordon, and S. E. Fitzwater (1991), The case for iron, *Limnol. Oceanogr.*, *36*, 1793–1802, doi:10.4319/lo.1991.36.8.1793.

McGillicuddy, D. J., L. A. Anderson, S. C. Doney, and M. E. Maltrud (2003), Eddy-driven sources and sinks of nutrients in the upper ocean: Results from a 0.1 degree resolution model of the North Atlantic, *Global Biogeochem. Cycles*, *17*(2), 1035, doi:10.1029/2002GB001987.

McGillicuddy, D. J., et al. (2007), Eddy/wind interactions stimulate extraordinary mid-ocean plankton blooms, *Science*, *316*, 1021–1026, doi:10.1126/science.1136256.

Measures, C. I., J. Yuan, and J. A. Resing (1995), Determination of iron in seawater by flow injection analysis using in-line preconcentration and spectrophotometric detection, *Mar. Chem.*, *50*, 3–12, doi:10.1016/0304-4203(95)00022-J.

Moore, J. K., and O. Braucher (2008), Sedimentary and mineral dust sources of dissolved iron to the world ocean, *Biogeosciences*, *5*, 631–656, doi:10.5194/bg-5-631-2008.

Moore, J. K., S. C. Doney, and K. Lindsay (2004), Upper ocean ecosystem dynamics and iron cycling in a global three-dimensional model, *Global Biogeochem. Cycles*, *18*, GB4028, doi:10.1029/2004GB002220.

Orsi, A. H., and C. L. Wiederwohl (2009), A recount of Ross Sea waters, *Deep Sea Res., Part II*, *56*, 778–795, doi:10.1016/j.dsr2.2008.10.033.

Orsi, A. H., W. M. Smethie Jr., and J. L. Bullister (2002), On the total input of Antarctic waters to the deep ocean: A preliminary estimate from chlorofluorocarbon measurements, *J. Geophys. Res.*, *107*(C8), 3122, doi:10.1029/2001JC000976.

Parekh, P., M. J. Follows, and E. A. Boyle (2005), Decoupling of iron and phosphate in the global ocean, *Global Biogeochem. Cycles*, *19*, GB2020, doi:10.1029/2004GB002280.

Prézelin, B. B., E. E. Hofmann, C. Mengelt, and J. M. Klinck (2000), The linkage between Upper Circumpolar Deep Water (UCDW) and phytoplankton assemblages on the west Antarctic Peninsula Continental Shelf, *J. Mar. Res.*, *58*, 165–202, doi:10.1357/002224000321511133.

Prézelin, B. B., E. E. Hofmann, M. Moline, and J. M. Klinck (2004), Physical forcing of phytoplankton community structure and primary production in the continental shelf waters of the western Antarctic Peninsula, *J. Mar. Res.*, *62*, 419–460, doi:10.1357/0022240041446173.

Raven, J. A. (1990), Predictions of Mn and Fe use efficiencies of phototrophic growth as a function of light availability for growth and C assimilation pathway, *New Phytol.*, *116*, 1–18, doi:10.1111/j.1469-8137.1990.tb00505.x.

Reddy, T. E., and K. R. Arrigo (2006), Constraints on the extent of the Ross Sea phytoplankton bloom, *J. Geophys. Res.*, *111*, C07005, doi:10.1029/2005JC003339.

Rose, J. M., et al. (2009), Synergistic effects of iron and temperature on Antarctic phytoplankton and microzooplankton assemblages, *Biogeosciences*, *6*, 3131–3147, doi:10.5194/bg-6-3131-2009.

Saito, M. A., T. J. Goepfert, A. E. Noble, E. M. Bertrand, P. N. Sedwick, and G. R. DiTullio (2010), A seasonal study of dissolved cobalt in the Ross Sea, Antarctica: Micronutrient behavior, absence of scavenging, and relationships with Zn, Cd, and P, *Biogeosciences*, *7*, 4059–4082, doi:10.5194/bg-7-4059-2010.

Sambrotto, R. N., A. Matsuda, R. Vaillancourt, M. Brown, C. Langdon, S. S. Jacobs, and C. Measures (2003), Summer plankton production and nutrient consumption patterns in the Mertz Glacier Region of east Antarctica, *Deep Sea Res., Part II*, *50*, 1393–1414, doi:10.1016/S0967-0645(03)00076-6.

Sarmiento, J. L., et al. (2004), Response of ocean ecosystems to climate warming, *Global Biogeochem. Cycles*, *18*, GB3003, doi:10.1029/2003GB002134.

Schlitzer, R. (2002), Interactive analysis and visualization of geoscience data with Ocean Data View, *Comput. Geosci.*, *28*, 1211–1218, doi:10.1016/S0098-3004(02)00040-7.

Schoemann, V., S. Becquevort, J. Stefels, V. Rousseau, and C. Lancelot (2005), *Phaeocystis* blooms in the global ocean and their controlling mechanisms: A review, *J. Sea Res.*, *53*, 43–66, doi:10.1016/j.seares.2004.01.008.

Sedwick, P. N., and G. R. DiTullio (1997), Regulation of algal blooms in Antarctic shelf waters by the release of iron from melting sea ice, *Geophys. Res. Lett.*, *24*(20), 2515–2518, doi:10.1029/97GL02596.

Sedwick, P. N., G. R. DiTullio, and D. J. Mackey (2000), Iron and manganese in the Ross Sea, Antarctica: Seasonal iron limitation in Antarctic

shelf waters, *J. Geophys. Res.*, *105*(C5), 11,321–11,336, doi:10.1029/2000JC000256.

Sedwick, P. N., T. M. Church, A. R. Bowie, C. M. Marsay, S. J. Ussher, K. M. Achilles, P. J. Lethaby, R. J. Johnson, M. M. Sarin, and D. J. McGillicuddy (2005), Iron in the Sargasso Sea (Bermuda Atlantic time-series study region) during summer: Eolian imprint, spatiotemporal variability, and ecological implications, *Global Biogeochem. Cycles*, *19*, GB4006, doi:10.1029/2004GB002445.

Sedwick, P. N., A. R. Bowie, and T. W. Trull (2008), Dissolved iron in the Australian sector of the Southern Ocean (CLIVAR-SR3 section): Meridional and seasonal trends, *Deep Sea Res., Part I*, *55*, 911–925, doi:10.1016/j.dsr.2008.03.011.

Smethie, W. M., and S. S. Jacobs (2005), Circulation and melting under the Ross Ice Shelf: Estimates from evolving CFC, salinity and temperature fields in the Ross Sea, *Deep Sea Res., Part I*, *52*, 959–978, doi:10.1016/j.dsr.2004.11.016.

Smith, W. O., and L. I. Gordon (1997), Hyperproductivity of the Ross Sea (Antarctica) polynya during austral spring, *Geophys. Res. Lett.*, *24*(3), 233–236, doi:10.1029/96GL03926.

Smith, W. O., J. Marra, M. R. Hiscock, and R. T. Barber (2000), The seasonal cycle of phytoplankton biomass and primary productivity in the Ross Sea, Antarctica, *Deep Sea Res., Part II*, *47*, 3119–3140, doi:10.1016/S0967-0645(00)00061-8.

Smith, W. O., M. S. Dinniman, J. M. Klinck, and E. Hofmann (2003), Biogeochemical climatologies in the Ross Sea, Antarctica: Seasonal patterns of nutrients and biomass, *Deep Sea Res., Part II*, *50*, 3083–3101, doi:10.1016/j.dsr2.2003.07.010.

Smith, W. O., Jr., and J. C. Comiso (2008), Influence of sea ice on primary production in the Southern Ocean: A satellite perspective, *J. Geophys. Res.*, *113*, C05S93, doi:10.1029/2007JC004251.

Smith, W. O., Jr., D. G. Ainley, and R. Cattaneo-Vietti (2007), Trophic interactions within the Ross Sea continental shelf ecosystem, *Philos. Trans. R. Soc. B*, *362*, 95–111, doi:10.1098/rstb.2006.1956.

Sunda, W. G., and S. A. Huntsman (1997), Interrelated influence of iron, light and cell size on marine phytoplankton growth, *Nature*, *390*, 389–392, doi:10.1038/37093.

Sweeney, C., D. A. Hansell, C. A. Carlson, L. A. Codispoti, L. I. Gordon, J. Marra, F. J. Millero, W. O. Smith, and T. Takahashi (2000), Biogeochemical regimes, net community production and carbon export in the Ross Sea, Antarctica, *Deep Sea Res., Part II*, *47*, 3369–3394, doi:10.1016/S0967-0645(00)00072-2.

Tagliabue, A., and K. R. Arrigo (2005), Iron in the Ross Sea: 1. Impact on CO_2 fluxes via variation in phytoplankton functional group and non-Redfield stoichiometry, *J. Geophys. Res.*, *110*, C03009, doi:10.1029/2004JC002531.

Takahashi, T., et al. (2009), Climatological mean and decadal change in surface ocean pCO_2, and net sea–air CO_2 flux over the global oceans, *Deep Sea Res., Part II*, *56*, 554–577, doi:10.1016/j.dsr2.2008.12.009.

Timmermans, K. R., L. J. A. Gerringa, H. J. W. de Baar, B. van der Wagt, M. J. W. Veldhuis, and P. L. Croot (2001), Growth rates of large and small Southern Ocean diatoms in relation to availability of iron in natural seawater, *Limnol. Oceanogr.*, *46*, 260–266, doi:10.4319/lo.2001.46.2.0260.

Timmermans, K. R., B. van der Wagt, and H. J. W. de Baar (2004), Growth rates, half-saturation constants, and silicate, nitrate, and phosphate depletion in relation to iron availability of four large, open-ocean diatoms from the Southern Ocean, *Limnol. Oceanogr.*, *49*, 2141–2151, doi:10.4319/lo.2004.49.6.2141.

Tortell, P. D., and M. C. Long (2009), Spatial and temporal variability of biogenic gases during the Southern Ocean spring bloom, *Geophys. Res. Lett.*, *36*, L01603, doi:10.1029/2008GL035819.

Tortell, P. D., C. Guéguen, M. C. Long, C. D. Payne, P. Lee, and G. R. DiTullio (2011), Spatial variability and temporal dynamics of surface water pCO_2, $\Delta O_2/Ar$, and dimethylsulfide in the Ross Sea, Antarctica, *Deep Sea Res., Part I*, *58*, 241–259, doi:10.1016/j.dsr.2010.12.006.

Twining, B. S., S. B. Baines, N. S. Fisher, and M. R. Landry (2004), Cellular iron contents of plankton during the Southern Ocean Iron Experiment (SOFeX), *Deep Sea Res., Part I*, *51*, 1827–1850, doi:10.1016/j.dsr.2004.08.007.

Wagener, T., C. Guieu, R. Losno, S. Bonnet, and N. Mahowald (2008), Revisiting atmospheric dust export to the Southern Hemisphere ocean: Biogeochemical implications, *Global Biogeochem. Cycles*, *22*, GB2006, doi:10.1029/2007GB002984.

A. M. Aguilar-Islas, School of Fisheries and Ocean Sciences, University of Alaska Fairbanks, 905 Koyukuk Dr., 245 O'Neill Bldg., PO Box 757220, Fairbanks, AK 99775, USA.

K. R. Arrigo and R. B. Dunbar, Department of Environmental Earth System Sciences, Stanford University, 473 Via Ortega, Rm. 140, Stanford, CA 94305, USA.

G. R. DiTullio, Grice Marine Laboratory, College of Charleston, 205 Fort Johnson, Charleston, SC 29412, USA.

M. C. Lohan, School of Earth, Ocean and Environmental Sciences, University of Plymouth, Portland Square, Plymouth P14 8AA, UK.

M. C. Long, National Center for Atmospheric Research, 1850 Table Mesa Dr., Boulder, CO 80305, USA.

C. M. Marsay, School of Ocean and Earth Science, University of Southampton, European Way, Southampton SO14 3ZH, UK.

M. A. Saito, Woods Hole Oceanographic Institution, 266 Woods Hole Rd., Woods Hole, MA 02543, USA.

P. N. Sedwick and B. M. Sohst, Department of Ocean, Earth and Atmospheric Sciences, Old Dominion University, 4600 Elkhorn Ave., Norfolk, VA 23529, USA. (psedwick@odu.edu)

W. O. Smith, Virginia Institute of Marine Science, College of William and Mary, Gloucester Point, VA 23062, USA.